2010

A Simulation Study of Factors that Affect Pressure Control During Kick Circulation in Managed Pressure Drilling Operations

Jose Eduardo Eduardo Chirinos
Louisiana State University and Agricultural and Mechanical College, jchirinos@gmail.com

A SIMULATION STUDY OF FACTORS THAT AFFECT PRESSURE CONTROL DURING KICK CIRCULATION IN MANAGED PRESSURE DRILLING OPERATIONS

A Thesis

Submitted to the Graduate Faculty of the
Louisiana State University and
Agricultural and Mechanical College
in partial fulfillment of the
requirements for the degree of
Master of Science in Petroleum Engineering

in

The Department of Petroleum Engineering

by
José Eduardo Chirinos
B.S., Universidad Central de Venezuela (U.C.V), Caracas, Venezuela, 2004
December, 2010

Acknowledgments

The author expresses special gratitude and appreciation to Dr. John R. Smith, whose ideas, suggestions and encouragement were of great value for the completion of this work. Also special thanks extend to Dr. Richard Hughes, Dr. Seung Kam and Darryl Bourgoyne for their kind acceptance to serve as members of the examination committee. The author is thankful to the LSU Craft & Hawkins department of petroleum engineering in general for giving the opportunity to complete this study under their supervision.

Special thanks to the members of the LSU MPD Consortium: At Balance™, Blade Energy Partners, Chevron Energy Technology Company, ConocoPhillips, Secure Drilling™-Weatherford, Total and Shell E & P, for supporting this research financially and technically. Acknowledgments are expended to SPT Group for providing academic licenses for the drilling simulator Dynaflowdrill™.

The author expresses his gratefulness to all his family members particularly, parents and brothers, for their spiritual support and continuous encouragement. Finally, special thanks to his wife who served as a source of support, love and inspiration during this project.

Table of Contents

List of Tables

List of Figures

Abstract

An university-industry consortium has been studying alternative well control procedures to be used for kicks taken during managed pressure drilling (MPD) operations using the constant bottom hole pressure (CBHP) method. The CBHP method of MPD allows more precise control of wellbore pressure than conventional drilling. MPD surface equipment allows more alternatives for controlling a kick and may support faster detection of kicks and losses which can reduce the severity of a well control event. Nevertheless, the elimination of well control incidents cannot be guaranteed, and the uncertainty in downhole drilling margins are not reduced by adopting MPD methods. The primary objective of this research was to evaluate pressure variation and maximum pressure during kick circulation to properly design and conduct a MPD operation.

Three specific objectives were addressed in this project. First, a pump start up method to keep bottomhole pressure approximately constant when beginning kick circulation after shut in is presented. Second, since formation pressure cannot be calculated by using shut in drillpipe pressure during typical MPD operations, a procedure to estimate kick zone formation pressure based on circulating pressure was documented. And third, a simple and practical method to estimate maximum expected casing pressure during well control operations was developed. This method was also used as part of a method for selecting kick circulating rate.

Methods for making calculations to achieve each of these objectives were developed. Computer simulations were used for comparison to a range of realistic well conditions. Full-scale gas kicks experiments were done to confirm applicability to a limited range of real situations. The applicability and accuracy of the method developed in this research were tested based on actual drilling practices reproduced in computer simulations and LSU well facility experiments.

Chapter 1 Introduction

1.1 General Description

A society relies on energy to develop and maintain its economic and social strength. Oil and gas are the main engines behind a society's growth, and their reserves depend on exploration and production practices. According to the Official Energy Statistics (EIA 2009), world consumption of oil and gas has increased about 40% and 100% respectively in the last 30 years (Figure 1.1). This increasing consumption trend has forced oil companies to explore for new reservoirs that can meet society's requirements in the future. In fact, new areas where information is limited are being explored in order to secure future energy demand. For example, during 2009, two important announcements were revealed about the deepwater area of the Gulf of Mexico (GOM): Tiber and Buckskin prospects. Tiber was drilled to a total depth of 35,055 ft, making it the deepest well ever drilled by the oil and gas industry, according to the operator (Lima et al. 2009).

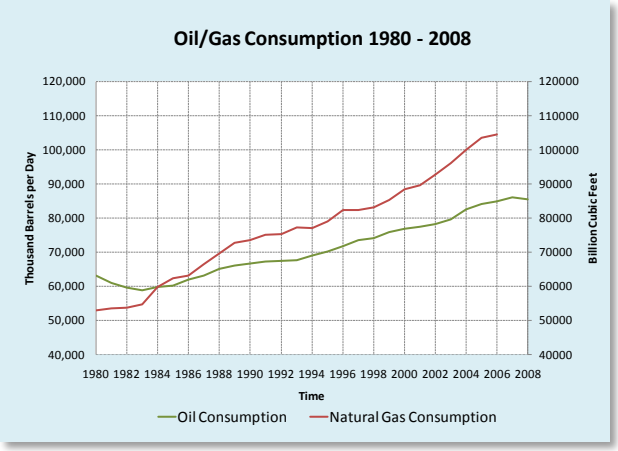

Figure 1.1 World Oil/Gas Consumption (EIA 2009)

According to the Mineral Management Service survey database, the drilling envelope in the GOM has increased significantly over the last 25 years. Figure 1.2 and 1.3 illustrate the trend in true vertical depth for deepwater wells and the trend in water depth for wells in the GOM. It can be seen how the oil and gas industry is drilling deeper wells in deeper waters (MMS 2009). These new areas

emerge with new challenges that increase both cost and operational hazards. Some of the challenges that drilling engineers have to face are: depleted zone in older fields, high pressures, high temperatures, narrow margin between fracture pressure and pore pressure, and others.

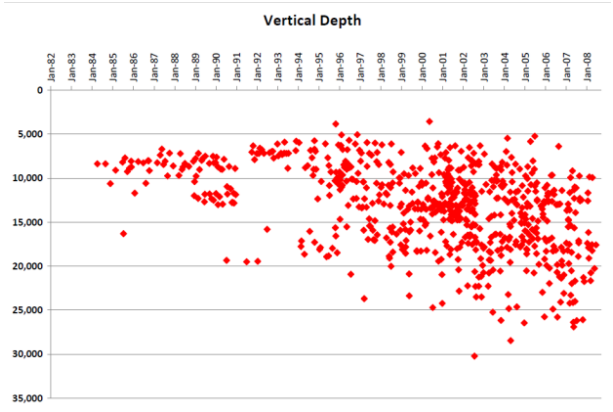

Figure 1.2 TVD trend for deepwater wells GOM (MMS 2009)

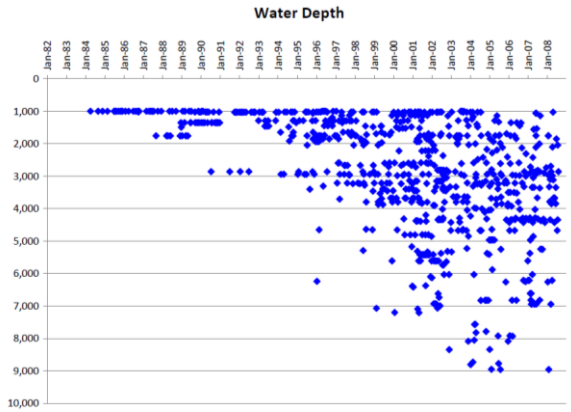

Figure 1.3 Water depth trend for wells GOM (MMS 2009)

Statistics related to drilling problems in the GOM published by James K. Dodson Company in 2004 have been used extensively by many authors; they all conclude that about 24% of the drilling operational time is non-productive time (NPT), and about 50% of the NPT is caused by pressure related problems. Grayson in 2009, based on Dodson's data, categorized pressure related problems that included well instability, low-pressure events and high pressure events, and he stated that the distribution for these groups were 18%, 22% and 12% respectably (Villatoro et al. 2009; Grayson 2009).

MPD Technology has come to play an important role in the oil and gas business by helping mitigate NPT and operational hazards. Technologies like underbalanced drilling (UBD) that completely replace many conventional elements of the drilling systems have been used by the oil industry in pursuit of better results. However, conventional drilling remains as the most common drilling technique by the oil industry due to practicality and lower cost. Unfortunately, conventional drilling is not an effective drilling technique where there is a narrow margin between pore pressure (PP) and fracture pressure (FP). Also, the overbalanced characteristic of conventional drilling has

proven to increase drilling cost because of low penetration rates in deep drilling environments. As a result, a new technology was developed called Managed Pressure Drilling (MPD).

According to the International Association of Drilling Contractors (IADC), MPD "is an adaptive drilling process used to precisely control the annular pressure profile throughout the wellbore. The objectives are to ascertain the downhole pressure environment limits and to manage the annular hydraulic pressure profile accordingly (IADC 2009)."

MPD uses many elements of conventional drilling and enhances the capability of the drilling system to control the operation in a more accurate way. This technology is based on well-bore pressure control, and its main purpose is to mitigate pressure related problems. Ideally well kicks, lost circulation and differential sticking are minimized, while the number of casing strings required to reach total depth is reduced. The main variations of MPD are: constant bottomhole pressure (CBHP), pressurized mud cap drilling (PMCD), dual gradient (DG), and health, safety and environment (HSE).

The focus of this project, and the most popular variation of MPD, is CBHP. This method uses a combination of equipment to manipulate annular frictional pressure losses and casing pressure to keep wellbore pressure constant. Although CBHP method of MPD has better control of wellbore pressure while drilling, well control events still occur because of uncertainty related to pore pressure and fracture pressure; in fact, MPD operations are often executed in highly uncertain environments, therefore the mitigation of well control incidents cannot be guaranteed. The overall objective of this project is the identification and evaluation of factors that need to be accounted for during the circulating phase of a well control event to properly design and conduct a MPD operation.

1.2 Objectives

CBHP operation of MPD should be designed in consideration of the worst possible scenario expected during operation. Different factors come into play when a drilling system is exposed to its limits. Such factors need to be managed to guarantee a safe and efficient drilling operation. This project focuses on the circulating phase of the well control event to assess elements that affect pressure variations during kick circulation. Three specific objectives were studied in this project. The first is to define a pump start up method for kick circulation after shut in; this method should keep bottomhole pressure approximately constant during pump manipulations. Since formation pressure cannot be estimated by conventional well control calculations during MPD operations, the second objective is to develop a way to estimate kick zone formation pressure based on circulating pressure. Finally, the last objective is to develop a method to predict casing pressure variations during circulation especially to 1) define a simple and practical method to determine maximum expected casing pressure during well control operations; 2) assess circulation effects on initial response selection; and 3) describe a method for selecting kick circulating rate.

1.3 Research Strategy / Plan / Method

This study is part of a larger research project conducted for the LSU MPD Well Control Consortium. The consortium provides technical advice and financial resources to identify "comprehensive and reliable well control procedures for CBHP method of MPD". The principal goal of this study is to complete a comprehensive assessment of the elements affecting pressure variation during circulation of a kick. The plan for accomplishing that goal is described in this section.

Methods for making calculations to achieve each of the objectives were developed. Computer simulations (Dynaflodrill™) based on actual drilling practices were used for comparison

to a range of realistic well conditions. Three different well geometries were used to simulate a broad range of scenarios: Well X, Well Y and LSU #2, hole sizes 6", 12 ¼" and 8 ½" respectively. Two initial responses were tested; one circulating response and one non-circulating response. In addition to this, different underbalanced situations, two or three kick sizes and two pump rates were used to complete a wide range of scenarios. Full scale experiments were also performed at the Petroleum Engineering Research and Technology Transfer Laboratory (PERTT Lab) at LSU; these experiments were done to confirm applicability to a limited range of real situations. The knowledge gained, conclusions, and recommendations were documented for transfer to sponsors, researchers conducting the remaining phases of the project, and the industry in general.

1.4 Overview of Thesis

Chapter 1 defines background and initial statement of the thesis; it explains the objectives of the research and gives overall introduction of the methodology used to achieve the thesis' objectives. Chapter 2 introduces the most important concepts of managed pressure drilling (MPD), and the constant bottomhole pressure method of MPD. Also, concepts and details of well control such as initial responses in MPD operations, kick tolerance, and pressure estimations during a well control event are described.

Chapter 3 describes the detailed methodology used to complete this research. It explains kick scenarios and well geometries used in full scale experiments and in computer simulations performed during the validation phase of this thesis.

Chapter 4 focuses on the pump start up schedule for use after a shut in during a MPD well control event. It describes the proposed procedure and demonstrates its applicability to real operations by showing a successful full scale experiment and computer simulations. Chapter 5 introduces a method to estimate formation pressure during a MPD well control operation based on circulating pressure. The results of applying this method to full scale experiments and computer

simulations are given. Chapter 6 introduces a new method to estimate the maximum casing pressure during kick circulation. This method is compared to single bubble calculation, full scale experiments and computer simulations. The results observed from these comparisons are discussed and analyzed. Finally, the kick tolerance concept is combined with this method to demonstrate its application in well planning.

Chapter 7 summarizes the most important conclusions of chapter 4, 5, and 6 and includes a list of recommendations for future work.

Chapter 2 Literature Review

2.1 MPD

Managed Pressure Drilling (MPD), is a relatively new technology developed to address drilling problems encountered during conventional drilling. According to the International Association of Drilling Contractors (IADC), "Managed Pressure Drilling is an adaptive drilling process used to precisely control the annular pressure profile throughout the wellbore. The objectives are to ascertain the downhole pressure environment limits and to manage the annular hydraulic pressure profile accordingly (IADC 2009)."

MPD uses different approaches to control and influence wellbore pressure. It is able to actively manipulate pressure profile by controlling back pressure, drilling fluid proprieties and circulating friction; hence, a combination of tools is used to achieve MPD objectives to reduce non productive time (NPT) and mitigate drilling hazards. MPD has been shown to have successful applications in wells were kicks, lost returns, ballooning, wellbore instability, and/or differential sticking caused excessive NPT or inability to reach the well's objectives using conventional drilling methods (Malloy et al. 2009; Hannegan 2006).

2.1.1 Applications and Benefits

Although the main application of managed pressure drilling is drilling in a narrow margin between pore pressure and fracture pressure, the oil industry has realized that MPD can be applied anywhere where more precise control of wellbore pressure is an advantage. As a result, the industry has already addressed significant number of challenges by using MPD. Some of the applications are: narrow drilling margin between pore pressure and fracture pressure, depleted formations, tight gas sands, shallow gas hazards, wellbore stability, fractured carbonates, HP/HT wells, H_2S wells, slim coiled tubing drilling and casing drilling.

The advantages of MPD include: reduce NPT, improves safety, increases rate of penetration, reduces formation damage, extends casing depths, reduces lost circulation and influx, eliminates stuck pipe problems, and increases wellbore stability (Hannegan 2006; Davoudi 2009; Arnone et al. 2009; Grayson 2009).

2.1.2 Methods of MPD

There are four methods of MPD described in the literature. Health, safety, and environment (HSE) is designed to isolate and avoid hazardous operations in the rig floor when toxic or high pressure fluids are being circulated out of the well. Pressurized mud cap (PMCD) refers to drilling without returns to the surface; its application is suited to handle severe lost circulation issues. The dual gradient (DG) method is used to control annular pressure by managing equivalent circulating density (ECD) in subsea areas where abnormally pressured zones are presented in narrow window between pore and fracture pressure. This method intends to modify the annular pressure profile by installing pumps on the sea floor or other means to give the effect of a higher pressure gradient below the sea floor from the seafloor up. A typical target case for DG drilling is the Gulf of Mexico deepwater drilling. Finally, the focus of this study, the constant bottomhole pressure method (CBHP) uses a closed annulus to keep relatively constant pressure at one point of the well. The main application is drilling in areas where pore pressure and fracture pressure margin is narrow (Rehm 2009; Nauduri et al. 2009; Hannegan 2006; Malloy 2008; Malloy et al. 2009).

2.2 CBHP Method of MPD

The constant bottomhole pressure (CBHP) method is the most common method of MPD. This method is designed to control wellbore pressure profile during drilling operations. During the application of this method, annular pressure in the well is held constant or near constant at a selected depth. CBHP actively controls the surface pressure using a drilling choke to compensate for

changes in frictional pressure losses (ΔP_{AF}) during routine operations such as making a connection. An important characteristic of this method of MPD is the minimization of wellbore pressure variation to keep wellbore pressure within the drilling margin. Consequently, it allows drilling within a narrower window, or margin, between fracture and pore pressures than conventional drilling methods.

2.2.1 Application of CBHP Method

CBHP uses a collection of tools to control wellbore pressure during drilling operation. The minimum equipment required to apply CBHP are a rotating control device (RCD), a drilling choke manifold (DCM) and a non-return valve (NRV). The RCD keeps annular space closed and diverts flow to the DCM; it is equipped with a rotating packer that rotates and holds pressure in the well during drilling operations. The DCM helps manipulate and control surface pressure while drilling; it can be controlled manually, semi-automatically, or automatically. A NRV or float valve is installed in the bottomhole assembly (BHA); it allows only downward flow of drilling fluids. There are other optional tools that can complement CBHP operation to improve wellbore pressure management such as coriolis meters (flowmeter), continuous circulating systems (CCS), downhole deployment valves, back pressure pumps, surface multiphase separators, pressure while drilling tools (PWD), and hydraulic flow modeling (Malloy 2008; Rehm 2009; Davoudi 2009).

Figure 2.1 shows an example of a pressure profile of a well where CBHP is being used, keeping BHP constant. For the dynamic line when rig pumps are on, BHP is a function of the mud density, the depth and the annulus surface pressure during circulation (blue line). However, when rig pumps are off, the CBHP method increases annular pressure (backpressure) to compensate for the lack of friction losses; consequently, BHP is then a function of the mud density, depth and the higher backpressure (solid red line). In other words, to prevent BHP fluctuation, a pressure equal to

the lost frictional pressure losses is applied at surface to keep BHP constant (Rehm 2009; Nauduri et al. 2009; Hannegan 2006; Malloy 2008; Malloy et al. 2009).

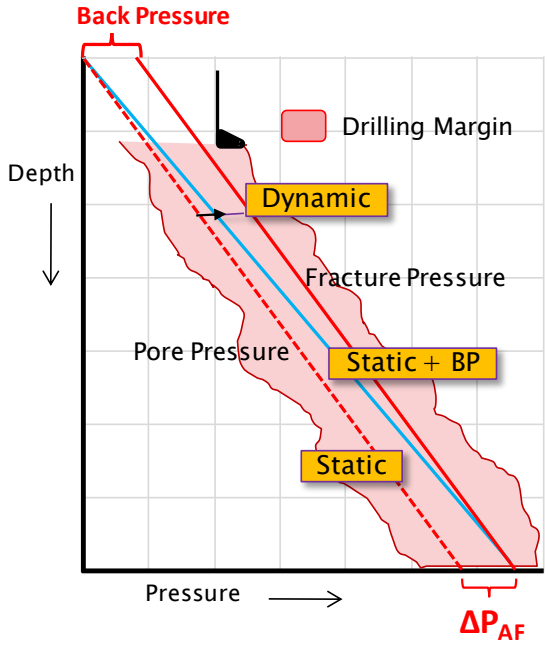

Figure 2.1 CBHP Method of MPD

2.2.2 Pump Shut down Schedule during CBHP Method

Many authors have discussed the method used to make a transition from dynamic to static state during CBHP method of MPD. Medley et al. (2008) and Rehm et al. (2008) described a method to achieve CBHP objectives when rig pumps are shut down. The method relies on a hydraulic model to estimate annular friction losses and equivalent circulating density (ECD) at different pump rates. Then, the ECD is manipulated by adjusting the casing pressure to keep wellbore pressure constant when the pump rate is reduced. Wellbore pressure and ECD estimation are made with hydraulic models, and they can be validated with pressure while drilling tools, if available. For example, to make a connection, the choke opening is reduced to increase casing pressure to the desired pressure, then the pump rate is reduced, thus surface pressure increases as the frictional pressure loss decreases by an equal amount. This process continues stepwise until the annulus surface pressure is at the maximum calculated value and the pumps are stopped. The final annulus surface pressure

should be equal to the frictional annulus pressure losses in the well during normal operation. Figure 2.2 illustrates how choke pressure should increase while pump rate is being reduced (Medley et al. 2008).

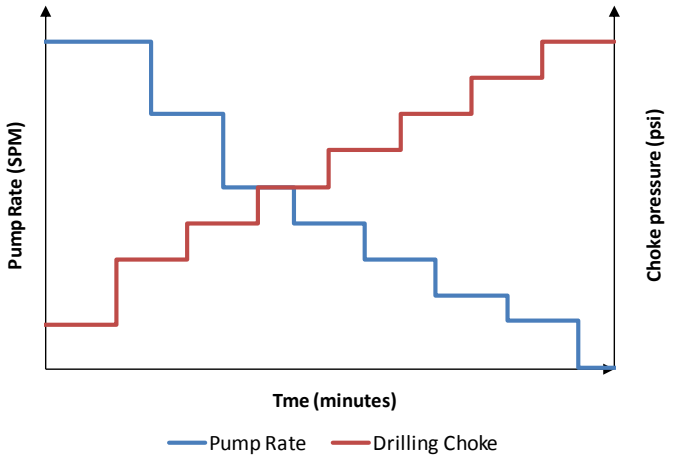

Figure 2.2 Pump rates/Choke pressures during connections

2.2.3 Initial Responses during Well Control Operation

A few studies have been done in the area of well control procedure for the CBHP method of MPD. In 2006, LSU created the MPD well control consortium to develop a basis for comprehensive and reliable well control procedures for the CBHP method of MPD. Das (2007) documented the first research from that consortium related to initial response comparison for CBHP. He compared three initial responses by using computer simulation: shutting in (SI) the well conventionally, increasing choke pressure while keeping the same pump rate, and increasing pump rate while keeping choke pressure constant. The most important conclusions from Das's research were: a) no single response was identified as the best, b) circulating responses may stop the influx faster than non circulating responses, c) increasing choke pressure response leads to a lower shoe pressure than SI, thus it reduces the risk of lost returns at the shoe (Das 2007; Das et al. 2008).

In 2009, Guner studied the most appropriate initial response and kick circulation method for an unexpected reduction of bottomhole pressure created by a surface equipment failure or unintended ECD reductions. Guner's conclusions explained that SI was the initial response that is

applicable for all kick scenarios; however, increasing choke pressure would generally be the most effective response when it was practical. For both responses, Guner recommended normal circulation rate (Guner 2009).

In 2009, Davoudi documented a complete research related to best initial responses to gas kicks taken during drilling operations with the CBHP method of MPD. He studied nine responses, five of them non-circulating responses and four circulating responses. The responses were compared based on the ability to stop formation flow, minimizing the risk of lost returns and additional kick influx, and the reduction of pressure imposed at surface and the casing shoe. Davoudi performed over 150 simulations. These simulations revealed that no single best initial response to all kicks could be identified. However, according to his research, three initial responses were demonstrated to have a broad application to different kick scenarios. The three initial responses were: a rapid increase of casing pressure until flow out equals flow in, a simple SI, and lastly, an adaptation of the MPD pump shut down schedule that allowed confirmation of low rate kicks. In addition, he concluded that the best initial response depended on well conditions and the equipment that is being used (Davoudi 2009; Davoudi et al. 2010).

Based on the LSU MPD consortium research, Davoudi et al. (2010) presented a proposed approach (Figure 2.3) for selecting initial responses during well control events for the CBHP method of MPD. They explained that one of the criteria in selecting the initial kick reaction must be the equipment available on site, specifically whether flow out metering was being used. In addition, according to this approach, the selection of the initial response should also consider the certainty of the well control event. As a final point, they explained that each initial response has key factors that need be considered to insure applicability and efficiency during the well control operations (Davoudi et al. 2010).

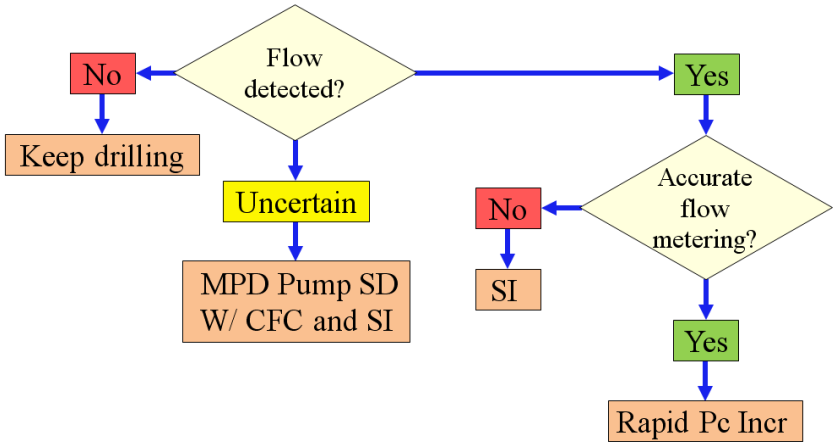

Figure 2.3 Proposed logic for selecting an initial response to kicks taken during MPD (Davoudi et al. 2010)

2.2.3.1 Flow Control Matrix

According to the Minerals Management Service (MMS 2008) a flow control matrix (FCM) is required to issue a drilling permit for MPD projects. The flow control matrix should provide rig crew instruction for different hazard levels; also, it should include comprehensible information to conduct a safe transition between normal drilling and well control operations. Figure 2.4 shows an example of a matrix used for the CBHP method. The inflow indicator is shown on the left side of the chart, and the pressure indicator (backpressure) is on the top part of the chart; both indicators have to be related to the maximum operational limits, and they need to be quantified to set different levels of alarm designated with different colors. Inside the chart, different measures reacting to the different alarm levels can be seen. Understandably, green areas in the chart represent routine drilling operations; conversely, red color represents the most hazardous conditions. In this case, the instructions are to pick up, shut in and evaluate the next action for the most hazardous conditions. Finally, flow control matrices are aimed to increase efficiency and awareness to hazard indicators. Nevertheless, the application of such matrixes depends on the experience of the crew and the rig equipment.

MPD Drilling Matrix	Surface Pressure Indicator			
	At Planned Drilling Back Pressure	At Planned Connection Back Pressure	> Planned Back Pressure & < Back Pressure Limit	≥ Back Pressure Limit
No influx	Continue Drilling	Continue Drilling	Increase pump rate, mud weight, or both AND reduce surface pressure to planned or contingency levels	Pick up, shut in, evaluate next action
Operating Limit	Increase back pressure, pump rate, mud weight, or a combination of all	Increase back pressure, pump rate, mud weight, or a combination of all	Increase pump rate, mud weight, or both AND reduce surface pressure to planned or contingency levels	Pick up, shut in, evaluate next action
< Planned Limit	Cease Drilling. Increase back pressure, pump rate, mud weight, or a combination of all	Cease Drilling. Increase back pressure, pump rate, mud weight, or a combination of all	Pick up, shut in, evaluate next action	Pick up, shut in, evaluate next action
≥ Planned Limit	Pick up, shut in, evaluate next action	Pick up, shut in, evaluate next action	Pick up, shut in, evaluate next action	Pick up, shut in, evaluate next action

Figure 2.4 Flow Control Matrix Example (MMS 2008)

Each operation is particular, which is why different matrices can be found in the literature. For example, in 2008 Viera et al. published a matrix based on influx gain and wellhead pressure (WHP). Urbieta et al. in 2009 based their matrix on influx state and WHP. Saponja et al. in 2006 used equipment maximum pressure rating (RCD, choke manifold and surface separators) to design their matrix. The initial response for each operation was different; they used increasing or decreasing backpressure, pump rate, and drilling fluid density (Saponja et al. 2006; Urbieta et al. 2009; Vieira et al. 2008).

2.2.3.2 Kick Circulation Methods

MPD circulating procedures have evolved from conventional well control. New approaches have been taken to reduce kick volume and improve kick detection; nevertheless, the same kick indicators are used during conventional drilling operations. Increased pit volume and increased mud return rate remain the primary indicators of an influx.

Similar conventional procedures to circulate a kick out of the well are used during MPD operations. All of them pursue the same objectives: prevent further kick entry, and circulate the kick out within the integrity limits of the formation, casing and surface equipment. During circulation,

backpressure at the choke is imposed to compensate for the loss in hydrostatic due to the kick fluid and the initial underbalanced situation. Thus, the main objective is achieved by maintaining constant bottomhole pressure (BHP) during the whole well control event (Watson et al. 2003).

The driller's method and wait and weight method are the most important conventional kill procedures in the oil industry. Both of them use drillpipe pressure to control BHP. The techniques are similar in many aspects, but the basic distinctions relate to when kill mud weight is pumped with respect to influx displacement. Driller's method uses the drilling fluid density that is currently available in the rig to displace the influx out of the well. Once the kick has cleared the wellbore, a heavier drilling fluid is circulated around the wellbore until the well is confirmed dead. The wait and weight method differs in that the heavier mud is mixed and pumped into the drillstring while the influx is still in the well (Bourgoyne 1991).

The kill procedure for a MPD operation uses the same principles as a conventional kill procedure. Section 2.2.3 mentions the two kinds of initial reactions to a kick during CBHP operation: non circulating and circulating. Both of them apply casing or choke pressure during circulation to increase BHP the same way that driller's method does. However, since the MPD circulating system is a closed system where choke pressure can be imposed during routine operations, the driller's method cam be applied promptly and may be concluded by only using additional casing pressure. Different technologies have been introduced that mainly allow the automation of the CBHP operation, these technologies use driller's method principles to keep BHP constant and circulate a kick out (Jenner et al. 2005; Santos et al. 2003; VanRiet et al. 2003; Reitsma 2005).

2.2.3.3 Well Control Case Histories

The CBHP method of MPD has been used extensively during recent years. Publications can be found related to the drilling problem events and the role of CBHP role during these operations. This

section discusses field experiences related to MPD application in places where drilling problems occurred.

Urbieta et al. (2009) showed the application of the CBHP method in a high pressure and high temperature (HPHT) field in Mexico. This field was known to have high reduced non-productive time (NPT) because of lost returns, well control events, stuck pipe and H_2S hazards. The authors explained that a lower dynamic overbalance was used with CBHP method, and NPT reduction was important. Also, they prepared a pump shut down schedule for routine operations to reduce BHP variation. Since the overbalance was minimal, small influxes were taken during operation. These were circulated out by circulating through a semi-automatic choke, and well shut in was not necessary (Urbieta et al. 2009).

Saponja et al (2006) discussed an MPD application in Canada. They explained that the MPD operations significantly reduced NPT caused by well control incidents. Continuous circulation with appropriate casing pressure adjustment was used during well control events. Consequently, drilling cost for these well decreased by 20%. Finally, they emphasized that a proper flow control matrix, as described in 2.2.3.1, should be in place to manage the risk and make decisions correctly during well control.

Reitsma (2010) discussed the importance of an early detection method during MPD operations. He discussed the uses of the flow meter (Coriolis meter) during kick identification and referred to the weakness of this kind of detection method. The author presented a simplified and effective method to indentify influx and losses during CBHP method of MPD. He explained that the standpipe pressure (SSP) and the annular discharge pressure (ADP) can be used for early detection when performing MPD with automated real time bottomhole pressure control using a surface choke. Reitsma also claimed that ADP and SPP can replace Coriolis meter, resulting in significant time and cost saving. Finally, he demonstrated the effectiveness of his method by

comparing real data from the well facility at LSU and Coriolis flow meter field data (Reitsma 2010; Reitsma et al. 2005).

Viera et al. (2008) discussed the application of MPD in an onshore exploratory well in Saudi Arabia. Experience in this field is characterized by unknown pore pressures, well control events and tight hole. The authors explained the uses of a semi-automated choke and a step wise pump schedule during routine operation. No well control events are described in this paper, however manipulation of the ECD was used to reduce high levels of connection and trip gas (Vieira et al. 2008).

Calderoni et al. (2006) described a case history in another exploratory well. He explained that conventional drilling was unable to make progress in the well because of the alternating gains and losses experienced. A side track was performed using CBHP method of MPD to avoid BHP fluctuations and maintain a minimum overbalance over the challenging area. Although a minimum BHP fluctuation was maintained, the change in ECD with depth affected the integrity of the well, and they experienced gains and losses during drilling. According to Calderoni (2006), after 14 days of working in the well, the well was controlled and completed. He stated that a complete understanding of the pressure behavior in the well is needed to have reliable well control procedures even during MPD operations (Calderoni et al. 2006).

2.3 Well Control Concept

The objective of the theory of well control and its practical application is to manage formation pressure. The main idea of well control involves all elements that interact over the wellbore pressure and keeps formation fluid out of the well. Despite the best practices during well planning, well control events keep happening, and MPD wells are not an exception. This section discusses the applicability of conventional drilling practices to MPD design and explains factors that need to be accounted for during MPD planning and operation.

2.3.1 Kick Tolerance

One aspect of this research relates to the expected casing pressure during circulation, and its implications for MPD operations. The kick tolerance concept is founded on the pressure boundaries that are encountered during drilling operations. According to Redmann (1991), the definition of kick tolerance is the "maximum increase in mud weight allowed by the pressure integrity test of the casing shoe with no influx". In other words, how much the mud density can be increased without breaking the shoe, assuming zero pit gain. A more proper description of this value is the zero gain kick tolerance. Other authors defined kick tolerance around kick volume stating that kick tolerance is the maximum volume of gas that can be circulated out of the well without exceeding fracture pressure of the weakest zone. A more relevant description of this value is a swabbed in kick tolerance (Spencer et al. 1999; Dedenuola et al. 2003). In 1995, Santos et al. defined kick tolerance more generally "as the capability of the wellbore to withstand the state of pressure generated during well control operations (well closure and subsequent gas kick circulation process) without fracturing the weakest formation." All definitions intend to quantify the limits of well control capabilities of the well during the planning phase.

2.3.1.1 Application

A significant number of companies currently use the kick tolerance concept during well planning and drilling operations. Its calculation is based on three parameters: the possible formation pressure at the depth of interest, maximum kick volume that can be taken during drilling, and the equivalent fracture density for the well (Santos et al. 1995).

If kick tolerance is being used for planning proposes, estimates of pore and fracture pressure and mud weight versus depth are needed. Formation pressure at the depth of interest and fracture pressure at the weakest zone can be read from the pressure profile built for the area. The maximum kick volume should be assumed according to a statistical approach that should include historical data

of the area; kick volumes on previous well control events can be used to guess kick tolerance (Redmann Jr. 1991). The main application of kick tolerance during planning phase is casing seat selection. The allowable kick tolerance is controlled by the maximum pressure that can be contained by the shoe or other weak section during a well control event. Consequently, the kick tolerance are the lesser of the values calculated when the well is shut in initially or when the gas influx reaches the deepest casing shoe. However, if kick tolerance is being used during the drilling, real data is used to determine whether the actual kick tolerance is adequate for drilling to continue. These calculations can be done on site, and usually they are performed by a computer program (Watson et al. 2003).

The kick tolerance calculation for shut in situation can be summarizes as follow:

A fracture pressure is used to estimate the maximum allowable annular surface pressure (MAASP) without exceeding the fracture pressure:

$$MAASP = FP - P_{hyd} \quad \text{(Eq. 2.1)}$$

Where FP = fracture pressure of the weak zone (most of the time casing shoe) and P_{hyd} is the hydrostatic pressure of the drilling fluid above the kick zone.

The maximum kick intensity that could be taken without fracturing a weak zone is usually called the "zero pit gain" kick tolerance; it is expressed as an equivalent mud density increase, and it is equal to the difference between the current mud weight and the maximum equivalent mud weight that could be used to kill a kick by shutting in at surface. This calculation assumes no pit gain as if the kick could be recognized and the well could be shut in instantaneously. Therefore, if the weak zone is assumed to be the casing shoe, the equation for zero pit gain kick tolerance, expressed in ppg, can be written as follows:

$$K_0 = \frac{(\rho_{frac} - \rho_{mud})\, D_{shoe}}{Depth} \quad \text{(Eq. 2.2)}$$

Where K_0 = kick tolerance with zero pit gain (bbl); ρ_{frac} = equivalent fracture pressure gradient (ppg); ρ_{mud} = mud density (ppg); D_{shoe} = casing shoe depth and $Depth$ = depth of interest (Redmann Jr. 1991).

Any fluid that is less dense than the drilling mud will cause a reduction of the hydrostatic pressure in the annulus, and a corresponding increase in casing pressure at surface. This increase can be expressed as:

$$\Delta P_{loss} = [(0.052\,\rho_{mud}) - g_{inf}]\; L_{inf} \qquad \text{(Eq. 2.3)}$$

Where ΔP_{loss} = loss in hydrostatic cause by an influx; L_{inf} = length of influx; g_{inf} = gradient of influx (usually 0.1 psi/ft is used for gas kick unless more precise information is known) (Redmann Jr. 1991).

Then kick tolerance expressed as underbalance (ppge) can be calculated as follows:

$$K_{inf} = \frac{MAASP - \Delta P_{loss}}{0.052\,Depth} \qquad \text{(Eq. 2.4)}$$

Where K_{inf}= kick tolerance due only to the effect of influx (Redmann Jr. 1991).

Kick tolerance is usually calculated for the initial shut in conditions. However, during the circulation phase of the well control procedure, expansion of the influx is necessary to reduce pressure in the influx and to keep bottomhole pressure constant. This expansion causes a loss in hydrostatic pressure that has to be compensated by an increase in surface and casing shoe pressure. Therefore, a different approach needs to be considered in order to determine maximum surface and shoe casing pressures during circulation. The next section will discuss a typical procedure to estimate annular pressure at any depth when a kick is in the well by using gas law.

2.3.2 Casing Pressure during Well Control Operations

Annular pressure prediction can be critical during well control incidents. A concern is the danger of fracturing a weak zone during the circulating phase of the well control operation that could lead to

an underground blowout in which uncontrolled flow of fluids from high pressure zones to the fractured zone occurs (Bourgoyne 1991). Thus, a proper well control strategy has to consider annular pressure variations during circulation of a kick while maintaining bottom hole pressure slightly above formation pressure.

The annular pressure profile during well control circulation depends directly on the kick composition. The density and expansion capability of the kick fluid influence expected annular pressure during circulation. For example, if the kick fluid is gas the expected peak casing pressure is higher than a liquid kick because of the gas expansion and the low density. The approximate kick density can be estimated from the observed drillpipe pressure, annular casing pressure and pit gain (Bourgoyne 1991).

2.3.2.1 Theoretical Calculation (Gas Kick)

The gas law and hydrostatic equations can be used in estimating annulus pressure, but some important assumptions have to be made: the influx enters the well and remains in a continuous slug or single bubble throughout the displacement; the gas remains in one phase and does not migrate or slip in the well; the influx is at the bottom of the drillstring when circulation begins; free gas behaves according to real gas law; and annulus frictional pressure losses are negligible. Figure 2.5 shows the schematic of a gas influx inside a well after displacement to surface casing shoe.

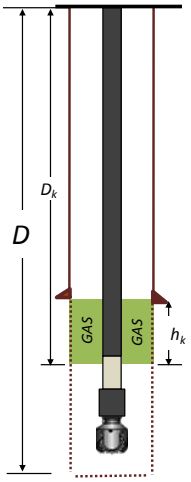

Figure 2.5 Schematic of well conditions during well control operations

The pressure at the top of the gas bubble (*p)* can be written as follow:

$$P = p_{bh} - g_{om}(D - h_k - D_k) - \Delta P \qquad \text{(Eq. 2.5)}$$

Where P = pressure at the top of a gas kick, p_{bh} = bottom hole pressure, ΔP = gas column hydrostatic pressure, D = total depth, g_{om} = mud gradient, h_k = gas kick height, and D_k = depth at top of gas bubble (Watson et al. 2003).

The hydrostatic pressure of the gas column is determined by multiplying its gradient by height. It can be expressed as follows:

$$P_{hg} = \frac{\gamma_g \, P \, h_k}{53.29 \, z \, T} \qquad \text{(Eq. 2.6)}$$

Where γ_g = specific gravity of the gas, z = compressibility factor and T = temperature. The influx height is the gas volume (V_k) at the depth of interest divided by the annulus capacity factor (C_a) (Watson et al. 2003). Since the number of moles in an influx does not change, its weight must be constant throughout the displacement. Thus, a relation between the initial gas column and the gas column anywhere in the well can be written as follow (Bourgoyne 1991):

$$P_{hg} = P_{hgi}\left(\frac{C_{ai}}{C_a}\right) \qquad \text{(Eq. 2.7)}$$

The gas volume is obtained from the gas law, and it can be written in term of gas height:

$$h_k = \frac{p_{bh} \, z \, T \, h_{ki} \, C_{ai}}{p \, z_{bh} \, T_{bh} \, C_a} \qquad \text{(Eq. 2.8)}$$

Finally, substituting terms into (Eq. 2.5) yield the quadratic expression,

$$p^2 - p\left(p_{bh} - g_{om}(D - D_k) - p_{hg}\right) - \frac{g_{om} P_{bh} z \, T \, h_{ki} C_{ai}}{z_{bh} T_{bh} C_a} = 0 \qquad \text{(Eq. 2.9)}$$

Solving for the equation root yields (Watson et al. 2003; Bourgoyne 1991; Vieira et al. 2009),

$$p = \frac{x}{2} + \sqrt{\left(\frac{x^2}{4} + \frac{g_{om} P_{bh} h_{ki} \, z \, T \, C_{ai}}{z_{bh} T_{bh} C_a}\right)} \qquad \text{(Eq. 2.10)}$$

Where the variable x is defined as,

$$x = p_{bh} - g_{om}(D - D_k) - p_{hg} \quad \text{(Eq. 2.11)}$$

The specific gas gravity must be known or assumed; a conservative approach is to use a 0.6 gravity gas. Also, note that the equation contains the compressibility factor at the depth of interest. As a result, it has to be adjusted to the desired pressure; this can be achieved by iterating z until calculation converge (Watson et al. 2003; Bourgoyne 1991; Vieira et al. 2009)).

2.3.3 Triangular Gas Distribution during Kick Circulation (Ohara 1996)

Ohara (1996) performed a number of full scale experiments at the LSU. He studied gas behavior in the wellbore during well control operations. Ohara's experiments demonstrated the existence of a triangular gas distribution in the well during gas kick circulation and proposed a triangular gas distribution profile (Figure 2.6)

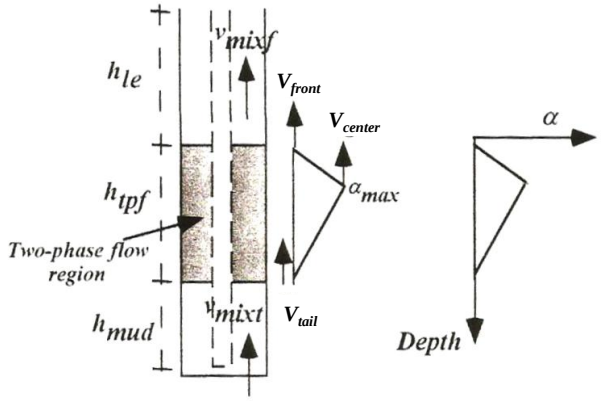

Figure 2.6 Proposed triangular gas distribution profile (Ohara 1996)

He explained that the triangular gas distribution profile is a function of the two-phase leading depth:

$$h_{le}(t) = h_{le}(0) - \int V_{front}(t)dt \quad \text{(Eq. 2.12)}$$

Where $h_{le}(t)$ = two-phase flow depth at time t; $V_{front}(t)$ = front edge velocity at time t

The length of the base of the triangle or the two-phase flow interval is given by:

$$h_{tpf}(t) = h_{tpf}(0) + \int [V_{front}(t) - V_{tail}(t)]dt \qquad \text{(Eq. 2.13)}$$

Where $h_{tpf}(t)$ = two-phase flow height at time t; $V_{tail}(t)$ = tail edge velocity at time t

Therefore, the average gas fraction can be defined as:

$$\bar{\alpha}(t) = \frac{Vol_{gas}(t)}{A_{an}h_{tpf}(t)} \qquad \text{(Eq. 2.14)}$$

Where $Vol_{gas}(t)$ = gas volume at time t; A_{an} = annular area. Notice that $t = 0$ means initial conditions.

Ohara explained that the gas will expand as it migrates upward, but its volume at standard conditions must be the same. This condition will change when gas reaches surfaces. After this, a mass balance must be applied to estimate the volume of gas that remains inside the well.

Ohara stated that each vertex of the triangle will move with different velocities and proposed velocity equations based on empirical data. According to his experimental results, the front velocity (V_{front}) will travel faster than the center velocity (V_{center}). Also, he observed the center velocity will travel faster than the tail velocity (V_{tail}). Finally, the equations for the front, center and tail vertex of the triangle when the superficial velocity of the liquid (V_{sl}) = 1.24 ft/sec are given by:

$$V_{front} = e^{1.767 - 2.953E-4*D} \qquad \text{(Eq. 2.15)}$$

$$V_{center} = e^{1.772 - 2.274E-4*D} \qquad \text{(Eq. 2.16)}$$

$$V_{tail} = V_{sl} \qquad \text{(Eq. 2.17)}$$

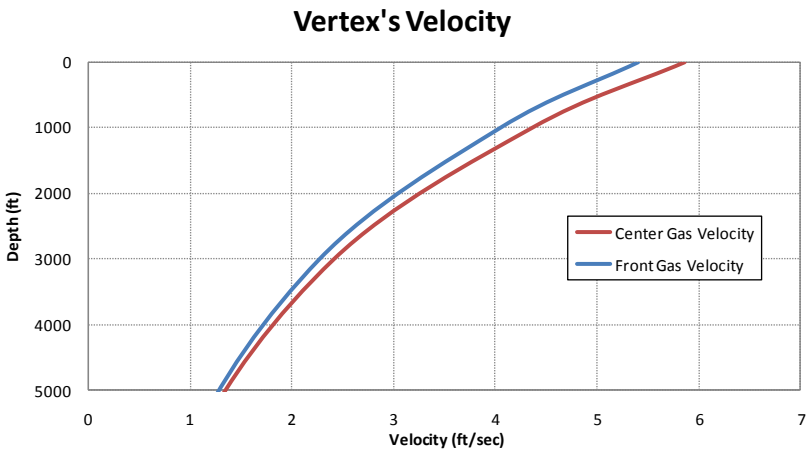

Figure 2.7 Graphical representation of the vertex's velocities

2.3.4 Estimation of Formation Pressure in Well Control Events

A conventional procedure when an influx is detected and confirmed is to shut in the well. This procedure prevents further entry of kick fluid into the well once the wellbore pressure reaches equilibrium with formation pressure. Usually, two pressure readings of the well can be seen: drill pipe pressure (SIDPP) and casing pressure (SICP). SIDPP can be used to estimate formation pressure as follows:

$$P_p = SIDPP + 0.052\,\rho_{mud}\,D \qquad \text{(Eq. 2.18)}$$

Where P_p= formation pressure (psi); ρ_{mud} = mud density (ppg); D = true vertical depth (ft) of the well.

Chapter 3 Research Methodology

3.1 General Plan

This project focuses on the circulating phase of a well control event during the CBHP method of MPD; it provides a basis to determine expected annulus pressure and compare to integrity limits related to equipment design and formation strength. In order to generate new knowledge about kick circulation in MPD operations, two approaches were used to study circulating factors: one involves full scale experiments (empirical data) conducted at the LSU Petroleum Engineering Research and Technology Transfer Laboratory (PERTT lab), and the other makes use of a variety of computer simulations performed using Dynaflowdrill™ as the main tool. The steps taken to conduct this research are detailed in this section:

1. **Current Knowledge**: literature related to MPD, gas distribution, kick circulation and well control in general were reviewed during this research. Particular emphasis was given to MPD well control operations since this concept is the core of this research. Empirical data and correlations developed by previous research were used.
2. **Simulations**: a multiphase transient commercial computer simulator (Dynaflodrill™) was used to simulate well control incidents in MPD operations.
3. **Well geometries**: one actual full scale well geometry and three simulated well geometries were used in this study. LSU #2 served as an experimental well where most of the full scale results of this research were measured and then compared to computer simulations. Two additional well geometries were used to perform several simulations based on the information provided by the sponsors of the LSU MPD consortium. Both wells have drilling environments suitable for MPD application: Well X is a 6" slim hole directional well with a potential deep kick zone whereas

Well Y is 12 ¼" straight hole with a potential high pressure sand at the bottom. A detailed description of both wells is provided in section 3.3

4. **Kick scenarios**: in order to study factors that come into play during kick circulation, one non-circulating and one circulating response were used to stop the influx during well control simulations (Figure 3.1). Also, at least two levels of circulating underbalance, two kick sizes and two circulating rates were used to evaluate pressure variations and to determine maximum pressure during kick circulation.

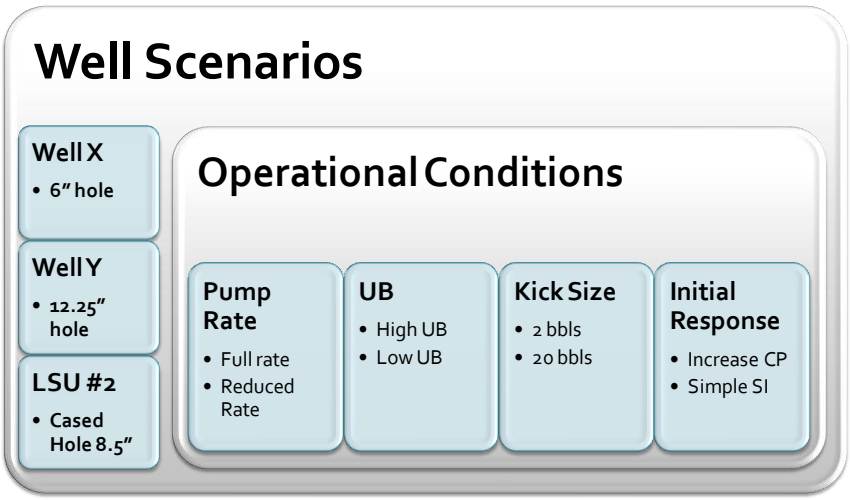

Figure 3.1 Simulated well scenarios

5. **Full Scale Experiment**: Data from several full scale experiments performed in the well LSU#2 (PERTT lab) in 1986 were used to validate and compare procedures developed in this project. The data contains more than ten full kick circulations performed under different conditions; Table 3.1 shows the main characteristics of these tests. It can be seen that four different mud rheologies were used in this project to generate a number of scenarios to compare. Also, the table shows that different pump rates were chosen to circulate the kick out; pump rates vary between 90 and 133 gpm. This data represents the main source of validation for this project because it emulates real operations; however, computer simulations were also used to compare results.

Table 3.1 Summary of tests with Water Base Mud (DEA Project 7 1986)

Test #	Mud Wt	PV	YV	10s/10m gels	Pump Rate (gpm)	Kill Circ Rate (gpm)
1-3	8.6	8	2	¾	90	90
1-4	8.55	8	2	4/4	90	133
1-5	8.6	7	2	3/2	133	90
2-2	8.75	24	19	20/14	0	90
2-3	8.7	23.5	22	21/15	90	90
2-4	8.7	24.5	23	20/16	90	118
2-5	8.7	25	19	21/17	106	90
3-2	12.5	22	5	9/6	0	90
3-3	12.3	20	4	8/6	87	90
3-4	12.4	20	3	8/6	90	94
3-5	12.4	19	4	9/6	110	90
4-2	12.35	37	13.5	19/13	0	90
4-3	12.4	35.5	14	19/12	88	90
4-4	12.3	33	13	17/15	86	133
4-5	12.3	32.5	12.5	18/12	110	90

3.2 Dynaflowdrill™

Dynaflowdrill™ (DFD) is a transient multiphase flow simulator used to simulate drilling operations. It was designed for underbalanced application; however, its interface allows MPD well control simulations as well. This tool runs under the Drillbench™ engine and includes an advanced multi-phase flow model that allows simulation of steady state and dynamic modes when formation fluid enters the well (SPT 2010).

There are diverse input data that should be collected before any drilling simulation can be performed. Some of the parameters required for DFD simulations are: well survey, well geometry, bottomhole assembly (BHA) specification, surface equipment, drilling fluid properties, and reservoir conditions. The pressure loss model, the friction factor model and supplementary observation points inside the simulated well were set according to the validation performed by Davoudi in 2009. An example of input data set is included in Appendix A.

Davoudi completed a comprehensive validation study for DFD in 2009. He performed more than 100 simulations and compared results with experimental data from two wells located at the PERTT lab: LSU #1 and LSU#2. He tested three different mud rheology models (Bingham, Power Law and Robertson-Stiff), two different pressure loss models (Mechanistic and Semi-empirical) and three different friction factor models (Colebrook, Dodge-Metzner, and Ed. Technip 1982), with four densities of water based mud from 8.6 to 12.4 ppg. According to Davoudi, DFD demonstrated acceptable simulation of steady state and transient condition versus real data for the models shown in Table 3.2.

Table 3.2 Results DFD validation study (Davoudi 2009)

Validation Study	Models Selected
Rheology Model	Robertson-Stiff
Pressure Loss Model	Semi-Empirical
Friction Factor Model	Dodge-Metzner

DFD has two options to control the simulations: interactive and batch modes. The interactive mode is characterized by flexibility during simulations; the user is able to modify operational parameter during simulation such as bit depth, pump rate, rate of penetration and choke opening. In batch mode, the simulation is set to follow planned steps before the simulation starts. In both cases the simulation results are viewed graphically during and after simulation, and they can be exported in the preferred format.

3.3 Wells Description

Three different well geometries were used to evaluate factors that are important during MPD kick circulation. LSU well #2 served as a source of real data as well as simulated data, and well X (6" hole) and well Y (12 ¼" hole) were used to simulate and test conclusions of this research.

3.3.1 LSU #2

LSU#2 is one of the wells located at PERTT lab in LSU. This well was used in simulations and in full scale experiments throughout this research. This is a vertical well which is 5884 ft deep and cased with 9 5/8" casing. The well is completed with a 1 ¼" gas injection line run concentrically in a 3 ½" drilling fluid injection line. The well also contains 2 3/8" perforated tubing which serves as a guide for well logging tools. Table 3.3 and Figure 3.2 illustrate well LSU#2 description.

Table 3.3 Well LSU#2 summary

Well type	Vertical experimental well
Reservoir fluid	Gas
Well profile	Vertical
Total Depth	5884 ft
Equivalent Hole size	8 ½" in
Bottom Hole Temperature (BHT)	109° F

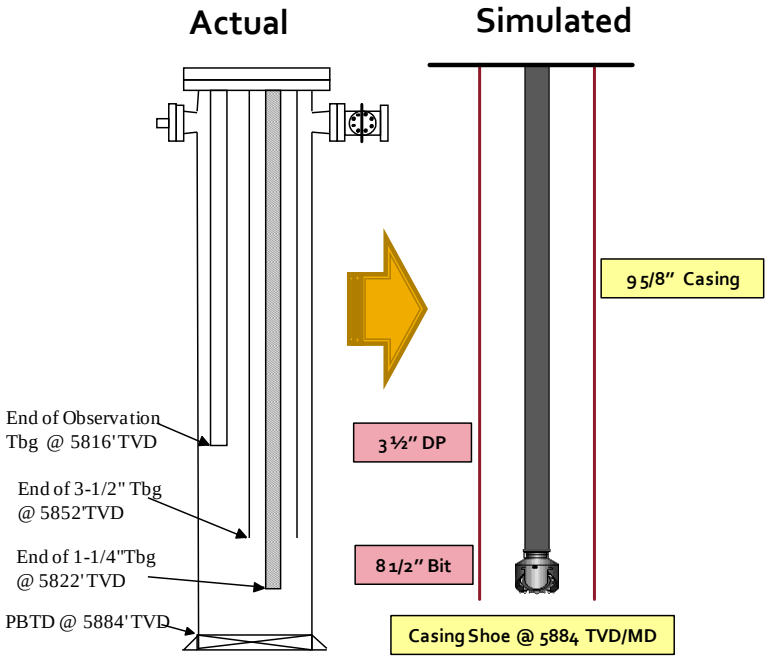

Figure 3.2 Well LSU#2 schematic actual/simulated

LSU #2 has been used in a significant number of research projects. In 1986, it was used in a project named DEA Project 7 to reproduce full scale kick circulation in water and oil based mud.

The recorded data of that project will be used to validate and compare procedures developed in this research.

Table 3.4 LSU#2 Operational settings

Pump Rate	90 - 195 gpm
Mud type	Water based mud
Mud Weight	8.6 – 12.3 ppg
Annular frictional pressure loss (P_{AF})	0 – 320 psi *

* A valve can be adjusted on the surface return line to simulate higher ΔP_{AF}

3.3.2 Well X

Well X is an offshore directional well that sidetracks from a window milled in an existing 7" liner. The BHA is composed of a 6" bit, 4 ¾" drill collars, and 3 ½" heavy weight drill pipe. The remainder of the drillstring is 3 ½" drillpipe. The milled window is at 15150 ft MD (13979 ft TVD) where the fracture gradient is 14.9 ppge. A high pressure sand is located at 16265 ft MD (14800 ft TVD) with pore pressure equal to 13.7 ppge. The total depth of the well is 17765 ft MD (15800 ft TVD). Table 3.5 and Figure 3.3 describe well X.

Table 3.5 Well X summary (Davoudi 2009)

Well type	Re-entry, sidetrack
Well objective	Produce from deeper sand
Reservoir fluid	Gas condensate
Well profile	Directional with max. 46° inclination
Rotary table elevation	170 ft
Water depth	2862 ft
Mud line	3032 ft
Top of window (shoe)	15150 ft MD (13979 ft TVD)
Total Depth	17675 ft MD (15800 ft TVD)
Hole size	6 in
Bottom Hole Temperature (BHT)	170° F
BHT (at shoe)	145° F

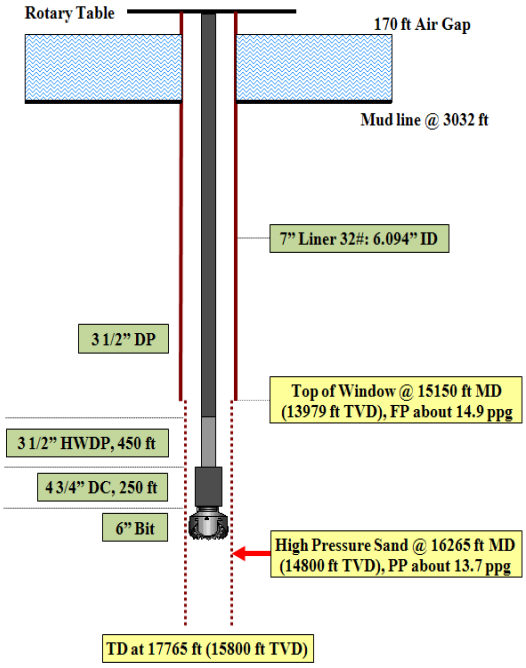

Figure 3.3 Well X Schematic (Davoudi et al. 2010)

This well is characterized by high annular friction pressure losses (ΔP_{AF}) even when the pump rates are low. Consequently, the expected ECD during drilling operation is about 1 ppge greater than the static equivalent mud weight (EMW), thus the risk of loss returns during drilling is significant. A meticulous MPD hydraulic design is needed to minimize BHP variation during routine operations. The operational parameters for well X are summarized in Table 3.6.

Table 3.6 Well X operational settings (Davoudi 2009)

Pump Rate	190 gpm
Mud type	Water based mud
EMW	13.2 ppg
Bit nozzles, total flow area (TFA)	4 x 11/32", 0.37 in^2
Drilling rate	60 ft/hr
Shoe fracture pressure	14.9 ppge – 10831 psi
ECD at shoe	13.75 ppge – 10000 psi
ECD on bottom	13.91 ppge – 10710 psi
Annular frictional pressure loss (P_{AF})	507 psi
High pressure sand	16265 ft MD (14800 ft TVD)
Maximum Allowable annulus surface pressure (MAASP) while circulating	831 psi

3.3.3 Well Y

Well Y is a large hole (12 ¼") offshore vertical well with a planned total depth of 15865 ft TVD. The BHA is composed of a 12 ¼" bit, 8" drill collars and 6 5/8" heavy weight drill pipe. The remainder of the drillstring is 6 5/8" drillpipe. 14" casing was set at 13780 ft TVD where the fracture gradient is 18.3 ppge. A high pressure sand is located at 14960 ft TVD with pore pressure equal to 17.3 ppge. Table 3.7 and Figure 3.4 describe well Y.

Table 3.7 Well Y summary

Well type	Large hole Vertical
Well objective	Produce from deeper sand
Reservoir fluid	Natural Gas
Well profile	Vertical
Rotary table elevation	150 ft
Water depth	100 ft
Mud line	250 ft
Casing shoe	13780 ft TVD
Planned Total Depth	15685 ft TVD
Total Depth for Simulations	14960 ft TVD
Hole size	12 ¼"
Bottom Hole Temperature (BHT)	200° F
BHT (at shoe)	193° F

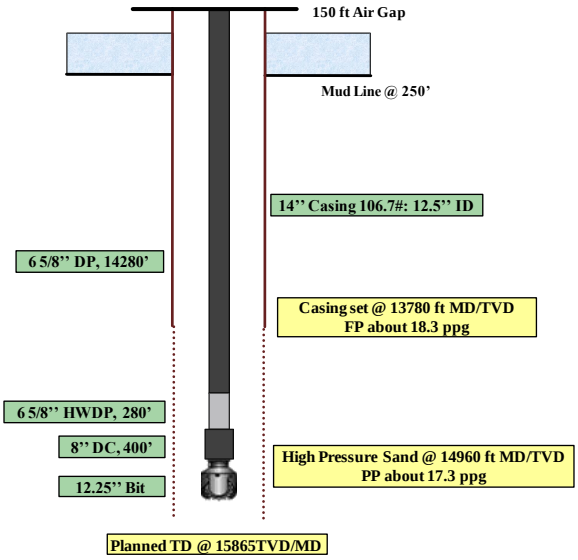

Figure 3.4 Well Y Schematic

Well Y is characterized by a narrow margin between pore pressure and fracture pressure which makes it a potential candidate for MPD applications. Some operational settings are listed in Table 3.8.

Table 3.8 Well Y operational settings

Pump Rate	760 gpm
Mud type	Water based mud
MW	17.3 ppg
Bit nozzles, total flow area (TFA)	13 x 11/32", 0.96 in^2
Drilling rate	60 ft/hr
Shoe fracture pressure	18.3 ppge – 13113 psi
ECD at shoe	17.54 ppge – 12573 psi
ECD @ 14690'	17.55 ppge – 13653 psi
Annular frictional pressure loss (P_{AF})	189 psi
High pressure sand	14960 ft TVD
Circulating Maximum Allowable annular surface pressure (MAASP)	539 psi

3.4 Well Kick Scenarios

3.4.1 LSU #2 Experimental Procedure

In the well LSU #2 well, drilling fluid was circulated down the annulus between the 3 ½" and 1 ¼" tubing at the desired pump rate, and the flow returns were taken through 3 ½" by 9 5/8" annulus. The gas kick was emulated by injecting gas in the 1 ¼" tubing at the desired injection rate until the desired pit gain was obtained. Subsequently, the planned initial response was applied to stop formation flow and circulate out the kick. The influx was circulated out through a mud gas separator where the gas was directed to the flare and the drilling fluid was returned to the mud pits.

Before the gas was injected, it was compressed in three storage wells located in the PERTT Lab facilities. The storage wells were cased with a 7" casing to 1900 ft, and essentially they were used as a gas reservoir. The wells were filled with gas at the beginning of an experiment from a connection to a natural gas pipeline. After that, water was pumped down through 2 3/8" tubing to

compress the gas inside the wells to the desired reservoir pressure. Figure 3.5 shows the experimental layout in PERTT lab.

During the experiments the drill pipe, casing and gas-injection pressures at the surface were continuously monitored and recorded. The pump rate, the gas rate in and out of the well, and the pit gain were measured and recorded. All the data was recorded in a personal computer where it can be manipulated and analyzed.

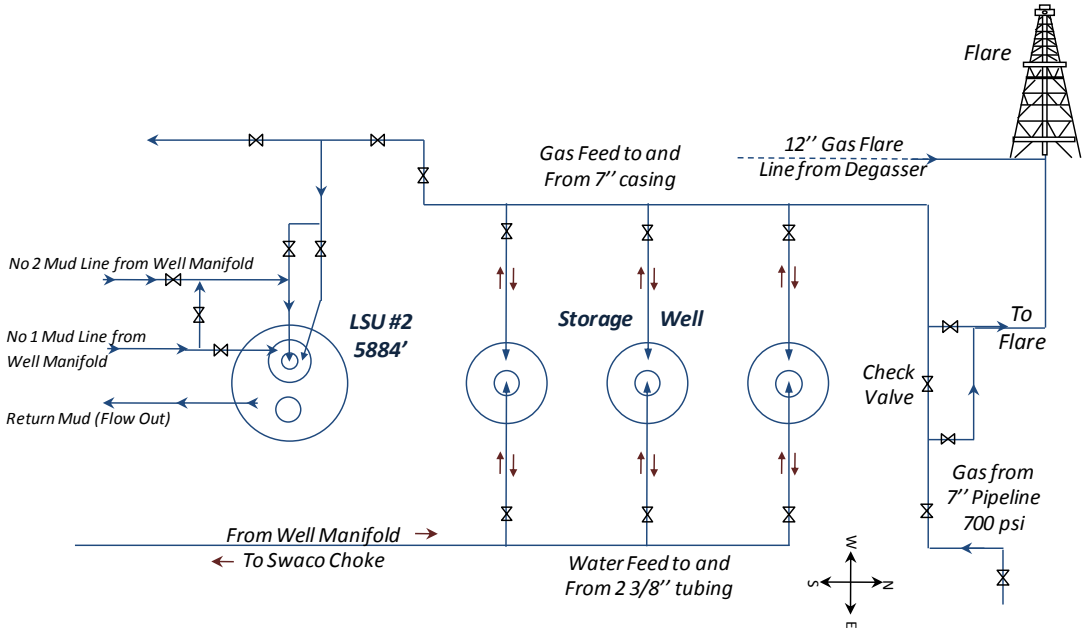

Figure 3.5 PERTT Experiment Layout

3.4.2 Simulation Procedure

The simulations in Dynaflowdrill™ start during drilling operations just above the high pressure (HP) sands in well X and Y. For LSU well #2, a high pressure sand was created in DFD to simulate real conditions. The bit would drill into the HP where a gas kick would be taken. Two initial responses are used to stop formation flow: increasing casing pressure (CP) and simple shut in (SI). If increasing casing pressure response is used, the kick would be circulated out without shutting in the well. However, if a simple shut in response is used, the well would be closed, and shut in casing pressure (SICP) recorded. Subsequently, this pressure is used to create a proper pump start up for kick

circulation. All simulations were carried out until the gas was completely out of the system; the data was recorded by DFD, and then manipulated in Excel. Figure 3.6 shows the two general sequential procedures used in DFD to stop formation flow and to circulate the kicks out.

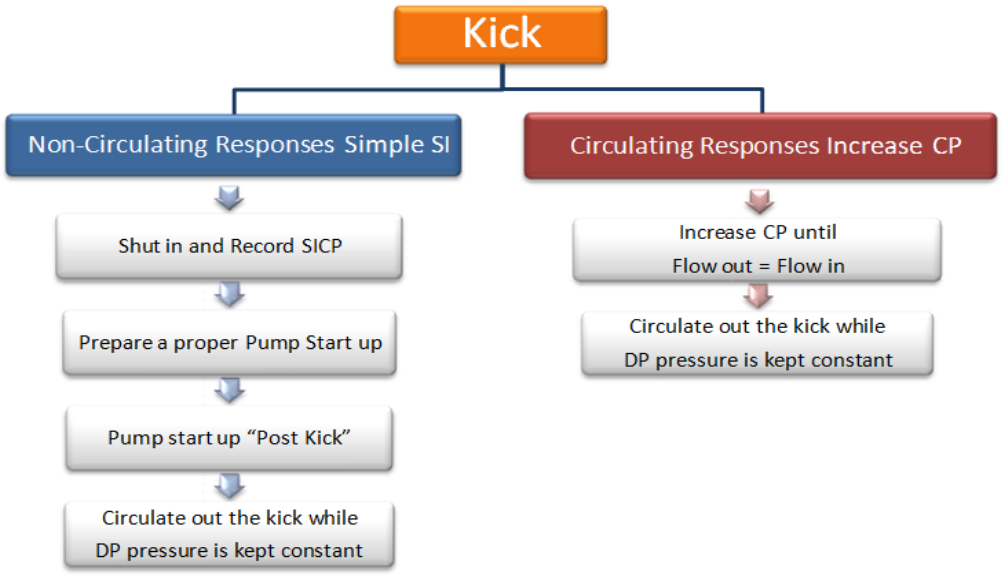

Figure 3.6 Initial Responses and general procedures

Different underbalanced circulating conditions and kick circulation pump rates were simulated in DFD to have a broad range of scenarios. Each simulation was performed for a total pit gain of 2, 10 and 20 bbl. Table 3.9 illustrates the different initial underbalanced circulating (UB) conditions and formation pressure (Pf) used during simulations.

Table 3.9 Simulated Kick Scenarios

	Well X (190 gpm)			Well Y (760 gpm)			LSU #2 (195 gpm)		
Static BHP (psi)	10186			13275			2617		
Circulating BHP (psi)	10706			13464			2942		
Friction (psi)	520			189			325		
Simulated Cases	**X1**	**X2**	**X3**	**Y1**	**Y2**	**Y3**	**L1**	**L2**	**L3**
P_f (psi)	10860	11289	11555	13606	14000	14245	3096	3525	3790
Static UB (psi)	674	1103	1369	331	725	970	479	908	1173
Circulating UB (psi)	154	583	849	142	536	781	154	583	848
Kick intensity (ppge)	**0.20**	**0.76**	**1.10**	**0.18**	**0.69**	**1.00**	**0.50**	**1.91**	**2.77**

Chapter 4 Pump Start up Schedule Method for Kick Circulation

4.1 Introduction

A total of 36 simulations in three different well geometries were performed in DFD. The simulations were evaluated based on BHP fluctuation during the pump start up after a simple shut in. Two circulating rates were tested to assess pressures during and after the schedules were applied. The simulations were recorded in DFD and analyzed in Excel, and the details are discussed in this chapter. Lastly, a full scale experiment was performed in the PERTT lab; it was used to validate the pump start up schedule procedure and to compare real data with simulated data.

4.2 Pump Start up Schedule after a Non-circulating Response

Pump start up and pump shut down procedures are routine MPD operations that are intended to keep bottomhole pressure relatively constant during pump manipulations (section 2.2.2). According to Davoudi (2009), one of the possible initial responses to a kick is simple shut in (SI). When this initial response is used the mud pumps are shut down and then the choke is closed as fast as is practical. The goal of this part of the research is to develop and evaluate a simple method to start the kick circulation and keep bottomhole pressure constant after a non-circulating response. The method would use information available on the rig to define a pump start up schedule.

Both non-circulating kick responses proposed by previous research (Davoudi 2009), shut-in and MPD pump shut down followed by a choked flow check and shut it, end with the well shut in; therefore this schedule is needed for both.

The method was evaluated using simulations as well as full scale experiments. The procedure used to test application of this method is summarized as follows:

1. The pump start up schedule for routine operation was defined. Table 4.1 shows a pump start up schedule with four steps of increasing pump rate, Q1 to Q4. As can be seen from the table, when the mud pumps are off the casing pressure (CP) is equal to the annular friction pressure loss (ΔP_{AF}) plus a desired casing pressure for routine operations (CP*). Notice that CP is reduced by a constant pressure increment (ΔP) at each step until it is equal to the CP*. This schedule keeps BHP approximately constant while the mud pump rate is increased. Note that a pump shut down would use this same schedule beginning at Q4 and reducing the pump rate.

Table 4.1 Pump start up schedule for routine operations

Mud Pump Rate	CP
0	**$CP_0 = \Delta P_{AF} + CP^*$**
Q1	$CP_0 - \Delta P$
Q2	$CP_0 - 2\,\Delta P$
Q3	$CP_0 - 3\,\Delta P$
Q4	**$CP^* = CP_0 - 4\,\Delta P$**

CP* = desired casing pressure for routine operations

2. A simulation was begun by drilling into the high pressure zone or by injecting gas into the experimental well (described in section 3.4.1). The well was observed until a kick was recognized; then drilling was stopped, the mud pump was shut down, and the choke was closed. Shut in casing pressure (SICP) was recorded until a stabilized SICP was interpreted.

3. Based on the stabilized SICP and the routine pump start up ΔP defined in step 1, a post kick pump start up schedule was defined for the MPD kick circulation. Table 4.2 illustrates a post kick pump start up schedule equivalent to the routine schedule presented in Table 4.1. It can be noticed that CP_0 is equal to SICP plus a desired safety overbalance factor (ΔP_{OB}), and the CP is reduced by the same ΔP and the flow rate increased to the same Q as defined for the routine pump start up.

Table 4.2 Post kick pump start up schedule

Mud Pump Rate	CP
0	$\mathbf{CP_{0\ Kick} = SICP + \Delta P_{OB}}$
Q1	$CP_{0\ Kick} - \Delta P$
Q2	$CP_{0\ Kick} - 2\ \Delta P$
Q3	$CP_{0\ Kick} - 3\ \Delta P$
Q4	$CP_{0\ Kick} - 4\ \Delta P$

4. The post kick pump start up schedule was applied to the simulations and the full scale experiments, and the kicks were circulated out completely by keeping drillpipe pressure constant (driller's method) when pump rate and choke pressure stabilized at Q4 and $CP_{0\ Kick}$- 4 ΔP respectively. BHP, CP and other parameters were monitored and recorded for discussion and analysis. The conclusions were based on the effectiveness of the method on keeping BHP constant, the applicability to real operations and the comparison with real data.

4.3 Simulation Results

Figure 4.1 shows a summary of the DFD simulations for each well geometry to test the pump start up method. All simulations were run successfully; BHP was kept almost constant during the initial phase of the kick circulation. An example of these simulations is explained in detail in the following section.

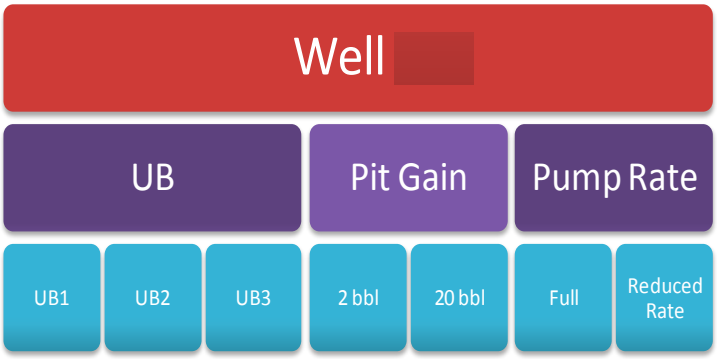

Figure 4.1 Well X simulations

4.3.1 Example Simulation of Pump Start up and Kick Circulation

Simulations were conducted to provide an example application of pump start up schedules. A pump start up schedule was defined to keep BHP constant during pump manipulations (Table 4.3). Figure 4.2 shows the simulation of the pump start up and pump shut down for routine operations for well X. It can be seen that BHP is kept almost constant while the pump is being started and shut down. Notice that casing pressure (CP) is used to compensate the loss of friction in the well; it is increased when pump rate (Pr) is reduced, and it is reduced when pump rate is increased.

Table 4.3 Well X pump start up normal conditions

Pr (gpm)	CP (psi)
0	522
10	457
43	407
80	357
105	307
121	257
137	207
152	157
166	107
179	57
190	14.7

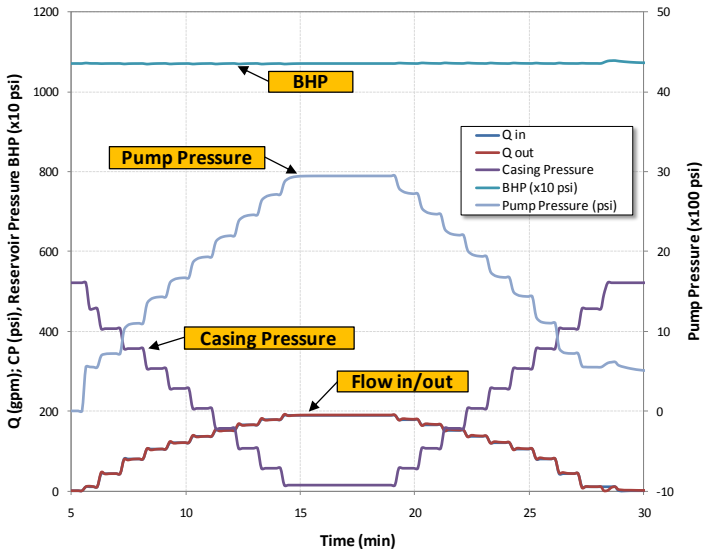

Figure 4.2 Pump start up normal conditions Well X

Once the pump start up schedule for routine operations was defined, the simulation was run according to the procedure described in section 3.4.2. The well drilled into a high pressure sand with a circulating underbalance of 0.2 ppg. As a result, a 20 bbl kick was taken, the well was shut in, and SICP was recorded. Based on the pump start up schedule for routine operations (Table 4.3) and the SICP, a new pump start up for kick circulation was built and the kick was circulated out successfully. The stabilized SICP was equal to 1183 psi. A safety margin or overbalance (ΔP_{OB}) of 100 psi was added to the SICP for determining the post kick start up schedule in Table 4.4.

Figure 4.3 demonstrates the application of the post kick pump start up. Table 4.4 shows how the beginning point of the post kick pump start up schedule is the sum of the SICP and ΔP_{OB}. Also, notice that casing pressure was reduced by the same ΔP used in the pump start up for routine operations. Figure 4.3 shows the simulation results for this scenario; a kick was recognized by the increase of surface mud flow rate out (Q_{out}), as shown by the red line. Drilling was stopped, the mud pump was shut down, and the choke was closed when pit level confirmed 20 bbls of gain. Casing pressure consequently increased to balance the kick zone's pressure at SICP = 1183 psi. Hence, the BHP increased and stopped formation flow. At this point, the post kick pump start up schedule was prepared and applied. Figure 4.3 demonstrates how casing pressure (purple line) was decreased while pump rate (red line) was increased according to the schedule in Table 4.4. Notice that BHP (light blue line) was kept almost constant during the application of this schedule; the maximum overbalance during the application of this schedule was approximately 230 psi.

Table 4.4 Pump Start up "Post Kick"

Pr (gpm)	CP (psi)
0	1283
10	1218
43	1168
80	1118
105	1068
121	1018
137	968
152	918
166	868
179	818
190	776

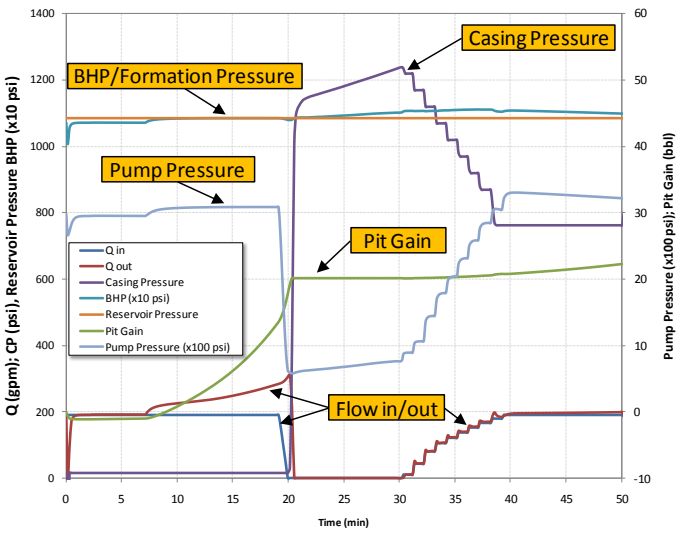

Figure 4.3 Pump start up application Well X 20 bbl 0.2 ppg Circ. UB FR

Figure 4.3 demonstrates the applicability of this method to start kick circulation after a non-circulating response. Notice that during planning phase, the desired overbalanced was 100 psi (ΔP_{OB}) for this post kick pump start up schedule; however, after running the simulation it can be observed that the overbalance values were between 100 – 230 psi. This fact can be attributed to three factors:

(1) gas migration after the well was closed for ten minutes, (2) gas traveling across different annular spaces because of the BHA components and (3) necessary fluctuation during choke manipulations. These events resulted in a higher CP, and therefore higher overbalance.

4.3.2 Full Rate vs. Reduced Rate

In order to study differences between full rate and reduced rate circulation, the same kick scenario discussed in the previous section (Well X, 20 bbl gain, 0.2 ppg circ. UB) was used to simulate a reduced rate circulation. Therefore, the method used was similar to the one discussed in section 4.3.1 with the only difference being that the circulating pump rate was 105 gpm. Figure 4.4 illustrates casing and pump pressure comparison for different circulating rates. Dashed lines represent full circulating rate pressures while solid lines correspond to reduced circulating rate pressures. It can be observed that casing pressure was higher and pump pressure was lower when reduced rate was used during circulation; this situation is attributed to the fact that there is less friction inside the well; therefore, more casing pressure is needed to keep BHP constant and above formation pressure.

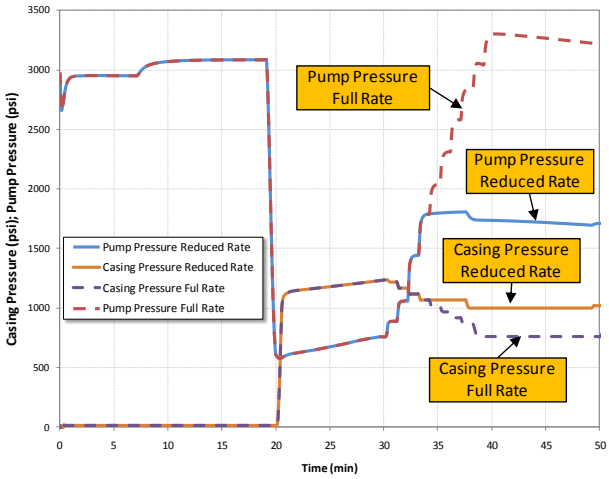

Figure 4.4 Casing/Pump pressure comparison full rate and reduced rate circulation

From Figure 4.4 it may be inferred that pump rate selection depends on surface equipment and formation strength. Surface equipment such as the rotating control device, pump relief valve

and separation equipment, in addition to formation limits such as leak off test and weak zone must be considered during kick circulating rate selection.

4.3.3 Full Scale Experiment

The method described was tested in a full-scale physical experiment in the LSU#2 well at the PERTT Lab at LSU. The drilling fluid used in the experiment was water, and the kick fluid was natural gas. The well was set to have conventional detection, and a restricted valve was used in surface return line to simulate higher annulus frictional pressure losses. The experimental results from the test were also compared to a computer simulation with the same conditions. The pump start up schedule for normal conditions is detailed in Table 4.5, and Figure 4.5 shows its application. Solid lines represent real data, and dashed lines correspond to simulated data.

Table 4.5 Pump start up normal conditions LSU #2

Pr (gpm)	CP (psi)
0	270
95	220
110	170
139	120
154	70
174	30

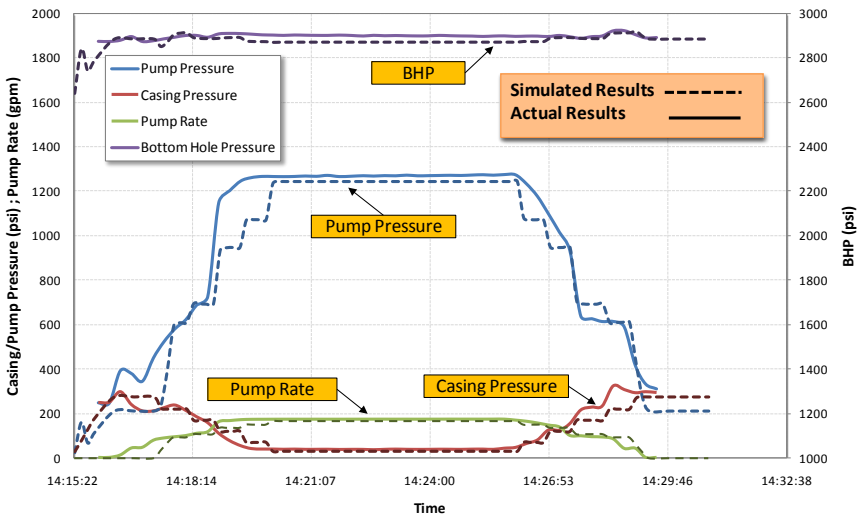

Figure 4.5 Pump start up normal conditions LSU #2

The full-scale experiment was performed according to the procedure explained in section 3.4.1. Gas was injected into the well until a 10 bbl kick was recognized, the well was shut in, and SICP was recorded versus time. The initial circulating underbalance was approximately 240 psi. Figure 4.6 shows drillpipe and casing pressure shut in build up; the stabilized SICP was estimated to be 510 psi. Table 4.6 illustrates the post kick pump start up built based on the pump start up for

normal conditions (Table 4.5) and the SICP. In this experiment, ΔP_{OB} was assumed to be equal to zero (0).

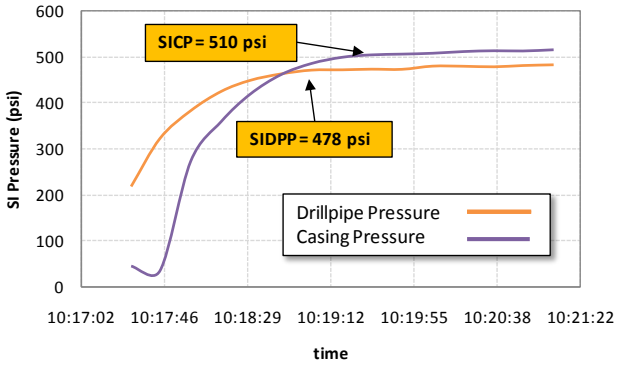

Figure 4.6 Shut in pressures Well LSU #2

Table 4.6 Pump start up post kick LSU #2

Pr (gpm)	CP (psi)
0	510
33	460
38	410
48	360
53	310
60	270

Once the post kick pump start up schedule was prepared, it was applied manually by two persons: one operated the pump and the other one manipulated the choke to control casing pressure. Figure 4.7 shows the experiment results. It can be observed from the graph, that BHP was kept almost constant during the kick pump start up, which validates the method described in section 4.2. Notice that the drillpipe and bottomhole pressure results from the experiment (solid lines) and the simulation (dash lines) are not identical for this case, probably because it was difficult to get exactly the same casing pressure versus time in the simulation as in reality, however the similarity in behavior supports the relevance of using simulations for this study.

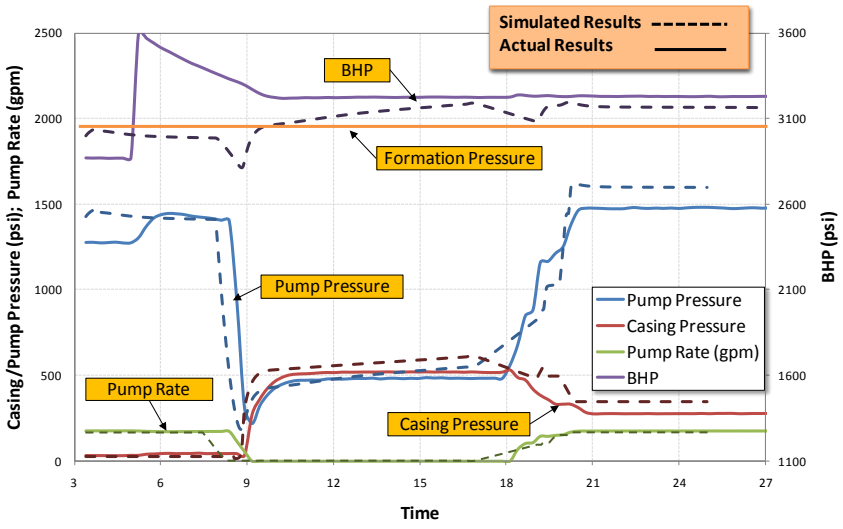

Figure 4.7 Pump start up full scale experiment LSU #2

4.3.4 Bottomhole Pressure Variation

The application of the pump start up method previously described generates an expected BHP fluctuation. A constant BHP depends on the right combination between mud pump rate and casing pressure during pump start up; therefore, BHP variation would depend primarily on the drilling crew's ability to follow the schedule correctly. Full-scale experiments and computer simulations were carried out emulating drilling operation to evaluate pressure variation during kick circulation. Figure 4.8 illustrates the BHP oscillation during pump start up for one full-scale experiment and six computer simulations in three well geometries. The vertical axis corresponds to the overbalance or safety margin (ΔP_{OB}) while the horizontal axis stands for time.

The first graph corresponds to two simulations in well Y. It can be observed that the fluctuation of ΔP_{OB} on 20 bbl kick is considerable higher than in 2 bbl kick. This difference can be attributed to the effect of choke pressure adjustment over the volume of gas inside the well. Also, it can be seen that ΔP_{OB} fluctuates approximately $\pm$ 25 psi, and up to 50 psi higher than intended, in the 20 bbl case. These variations correspond to the compressibility of the gas and choke adjustment imposed on surface which were 50 psi according to the schedule. It is clear that every time that the choke pressure was adjusted, ΔP_{OB} increased, and therefore BHP increased too.

The second graph refers to simulations in well X; it can be observed that ΔP_{OB} fluctuates similar to well Y. However, the ΔP_{OB} tendency is also affected by the well geometry of the well. This well has a slim hole, thus BHP is sensitive to the flow area variation around the BHA. The disparity of flow areas between drill collar (DC) and open hole (OH), and drillpipe (DP) and open hole creates a BHP variation that does not depend on the pump start up or choke manipulation. When the gas kick is moving in front of the DC, it spreads in the annular space occupying a longer section of the well, which results in a lower BHP. After the gas moves above the DP, it occupies a shorter section of the well that results in the BHP being slightly higher than was intended.

The third and fourth plots correspond to computer simulations and a full scale experiment in well LSU #2. Although, it can be observed that ΔP_{OB} fluctuates around the desired safety overbalance, the ΔP_{OB} variations in these cases were not of the same magnitude as in the well X and well Y simulations. This result is attributed to the difference in total depth between the wells; well X and Y are over 14000' deep whereas LSU#2 is 5884'. The choke adjustments during pump start up in LSU#2 are observed on bottom faster than in the other two wells, therefore, there is no delay in keeping BHP constant. Finally, according to the experiment and simulation results the best approach to control BHP with less variation than ΔP steps is by not forcing the well to conditions at a specific step but using the schedule as a dynamic target.

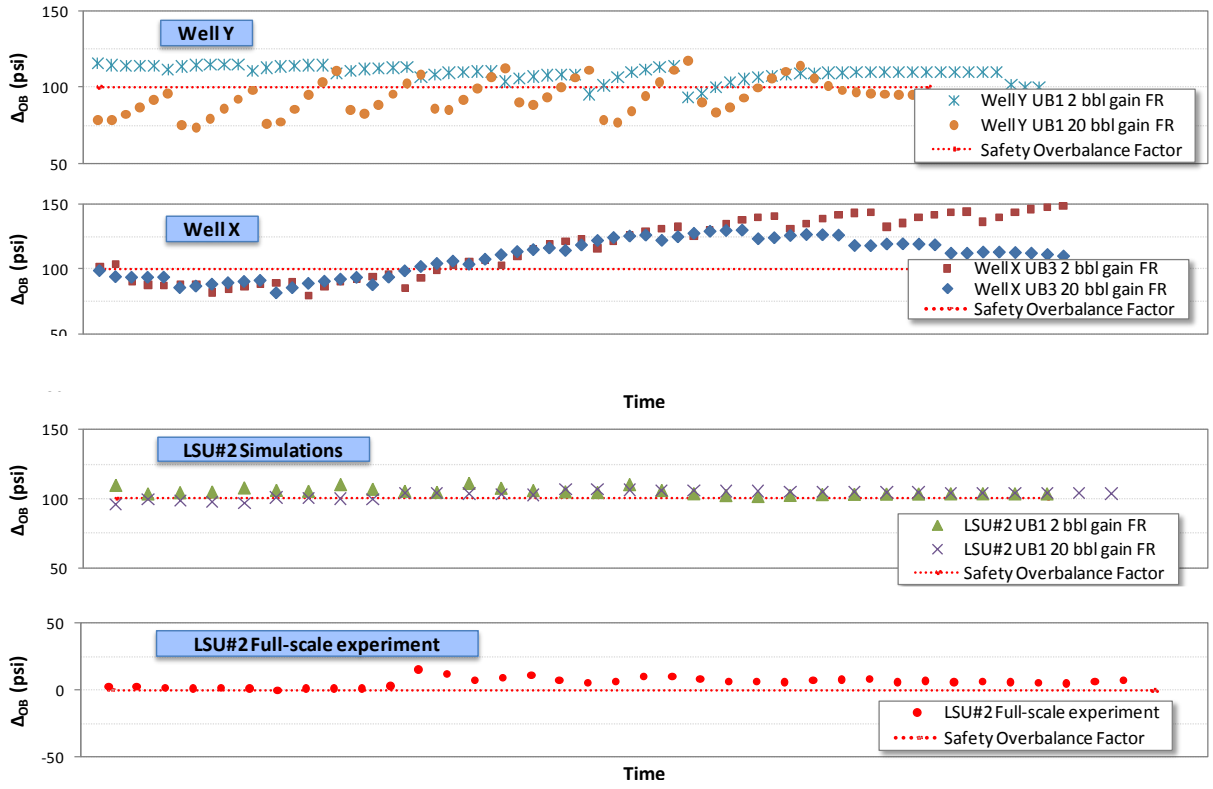

Figure 4.8 BHP variation during pump start up

4.4 Summary and Conclusions

The pump start up schedule method described in this chapter proved to keep bottomhole pressure relatively constant during pump start ups for kick circulation. It is applicable after all non-circulating response, and it can be summarized as follows:

1. Record and interpret a stabilized shut in casing pressure (SICP) after a non-circulating response.
2. Create the post kick pump start up schedule:
    a. Initial casing pressure equal to stabilized SICP plus a desired safety overbalance (ΔP_{OB}).
    b. Use the same pump rate steps as the normal pump start up.
    c. Reduce casing pressure by the same ΔP used in the schedule for normal conditions
3. Apply the schedule and then circulate out the influx keeping drillpipe pressure constant once it has stabilized after start up.

Kick circulating rate should be defined considering limitations on equipment and formation strength. It was proved that full circulating rate would demand higher pump pressure and more separation capacity on surface, whereas reduced pump rate would create higher casing pressures which affect weak formations e.g. exceed fracture pressures, and surface equipment such as the rotating control device.

Finally, there are other considerations that need to be accounted for when this method is applied. It was observed that bottomhole pressure typically varies ± 25 psi while the post kick pump start up schedule was being applied. BHP fluctuation can be minimized by having a well trained drilling crew, which is important for this kind of operations, or by utilizing automated system to

manipulate choke pressure. In addition, the safety overbalance factor (ΔP_{OB}) definition should consider gas migration effects when the shut in period is long; in other words, it is important to have a good interpretation of the SICP to avoid unintentionally applying an excessive ΔP_{OB} during kick circulation. All these factors are especially important to consider if dealing with narrow margins between pore pressure and fracture pressure.

Chapter 5 Formation Pressure in MPD Operations

5.1 Introduction

The estimation of formation pressure is very important during well control events; it is often a key to prevent further well control situations. The conventional method to estimate formation pressure involves shutting in the well to get drillpipe pressure readings (SIDPP). However, MPD operations typically require the use of a non return valve (NRV) in the BHA which impedes formation pressure estimation by this conventional method. Hence, a different procedure to determine formation pressure is needed. This chapter describes, applies and compares a method to estimate formation pressure based on circulating pressures and bottomhole pressure. Computer simulations and a full scale experiment are presented to validate the proposed MPD formation pressure estimation method.

5.2 Procedure

MPD operations generally require the use of a non return valve (NRV) in the BHA. A NRV allows only downward flow of drilling fluid, thus it does not allow valid SIDPP readings. Also, one of the three preferred initial responses during CBHP method of MPD does not include shutting in the well. Hence, a different procedure to determine formation pressure is needed.

Kick circulation pressure differs from static condition mainly because of the annular friction losses. Different models can be applied to estimate frictional pressure losses in the well, and validation processes can be done on site if pressure while drilling tools are present in the operation. Then, BHP and drillpipe pressure are known for given circulating rate, mud property and casing pressure.

While drilling, BHP can be estimated from drillstring information; hence BHP_o for routine operation is defined as:

$$BHP_o = P_{dpc\,o} + P_{hyd} - \Delta P_{ins} \quad \text{(Eq. 5.1)}$$

Where P_{dpc} = circulating drillpipe pressure or pump pressure; ΔP_{ins} = pressure loss inside the pipe (surface equipment, drillstring and bit).

If BHP_o is less than formation pressure in a permeable zone, a kick would occur. Consequently, additional casing pressure would be needed to increase BHP to balance formation pressure. Thus, the BHP_{inf} to stop formation flow after a kick is taken can be written as:

$$BHP_{inf} = P_{dpc\,inf} + P_{hyd} - \Delta P_{ins} \quad \text{(Eq. 5.2)}$$

Where $P_{dpc\,inf}$ = circulating drillpipe pressure after kick is controlled. Notice that it is assumed that the mud weight and the pump rate are constant, and therefore the friction in the well does not change significantly.

When a well control procedure is executed, BHP is kept constant while the influx is circulated out of the well. Therefore, we know that formation pressure (P_p) is equal to BHP_{inf} to stop formation flow; and this can be expressed as:

$$BHP_{inf} = P_p \quad \text{(Eq. 5.3)}$$

Finally, if Eq. 5.1, Eq. 5.2, Eq. 5.3 are combined the formation pressure can be expressed as:

$$P_p = P_{dpc\,inf} - P_{dpc\,o} + BHP_o \quad \text{(Eq. 5.4)}$$

5.3 Simulation Results

5.3.1 Computer Simulations

The computer simulation results were divided in two groups: the non-circulating and the circulating responses. Formation pressures were estimated based on the procedure described in section 5.2 and compared to the formation pressure set in the simulator.

5.3.1.1 Non-circulating response

Figure 5.1 shows simulation results after a non-circulating response (simple SI) to a 20 bbl kick in Well X; the circulating UB was 0.2 ppge. Following the SI, a proper pump start up was applied, and full pump rate was used circulated the kick out; the ΔP_{OB} used was 100 psi. The procedure described in section 5.2 was applied to estimate and compare reservoir pressure. As can be read from the graph, BHP_{BK} was 10706 psi before the kick and the drillpipe pressures before (DPP_{BK}) and after kick (DPP_{AK}) were 2950 psi and 3200 psi respectively. Table 5.1 illustrates the application of the method previously described; notice that formation pressure was estimated to be 10856 psi which is a good approximation to the actual formation pressure set in the simulator (10860 psi).

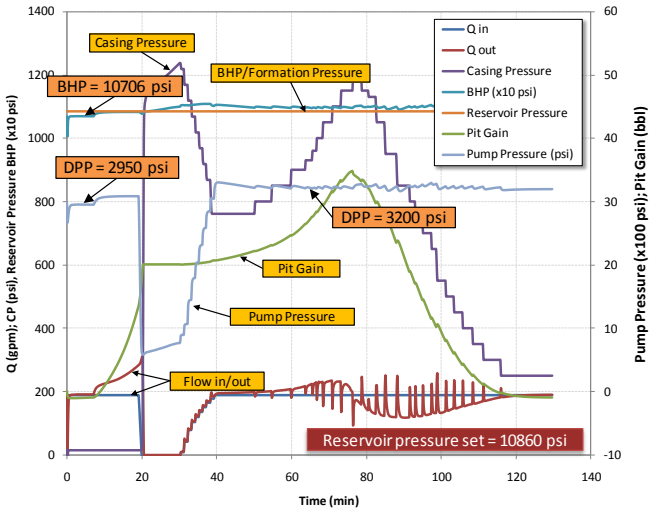

Figure 5.1 Well X full circulation

Table 5.1 Well X formation pressure

BHP_{BK}	+ 10706 psi
DPP_{AK}	+ 3200 psi
DPP_{BK}	- 2950 psi
ΔP_{OB}	- 100 psi
Estimated Reservoir Pressure	**= 10856 psi**

From Figure 5.1 and Table 5.1, it may be concluded that this estimation method of formation pressure relies on the correct BHP evaluation before the influx and the true ΔP_{OB} during kick circulation. BHP evaluation depends on an accurate frictional pressure loss model or PWD readings. On the other hand, the true ΔP_{OB} during circulation after a non-circulating response depends on the correct reading of the SICP; if an incorrect SICP is read, the casing pressure during circulation would probably be higher than what is really needed; and consequently, ΔP_{OB} would be more than it is intended to be.

5.3.1.2 Circulating response

A similar approach was applied to simulation results after a circulating response (increased CP) to a 20 bbl kick in Well Y; the circulating UB was 0.57 ppge. After the kick was detected, the choke was rapidly closed to match flow in and flow out, and then two additional adjustments were performed to ensure that the influx was stopped. The expression Eq. 5.4 was applied to estimate reservoir pressure and compare with the actual reservoir pressure set in the simulator. In circulating responses, special attention needs to be placed on the safety margin or overbalance (ΔP_{OB}) used; ΔP_{OB} would be determined by the casing pressure imposed by the drilling choke operator when the kick is being controlled, and its value depends on the number of adjustments made after flow in matches flow out for the first time. Figure 5.2 illustrates the simulation result for the case described above. Notice that after the influx was stopped, two choke adjustments were made. As a consequence, casing pressure increased by 128 psi; this value represents the ΔP_{OB} applied to circulate the kick out. Also, it can be observed that BHP_{BK} was 13557 psi, and DPP_{BK} and DPP_{AK} were 3725 psi and 4291 psi respectively. Table 5.2 shows the application of the method discussed in this chapter. Observe that reservoir pressure was estimated to be 13995 psi, and the actual reservoir pressure was set to 14000 psi; thus, the formation pressure calculation error was -5 psi, much less than 0.1%.

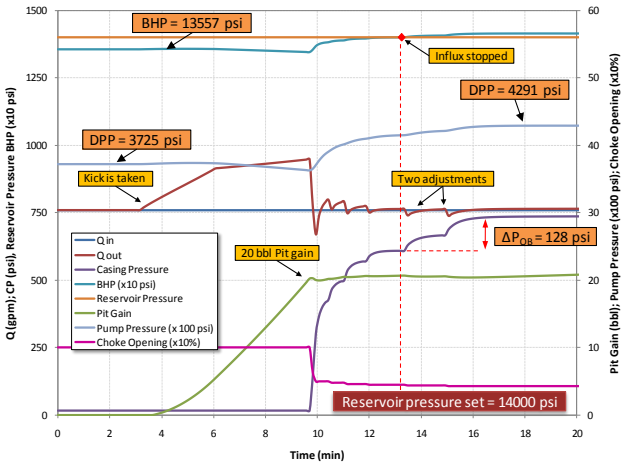

Figure 5.2 Well Y circulating response

Table 5.2 Well Y formation pressure

BHP_{BK}	+ 13557 psi
DPP_{AK}	+ 4291 psi
DPP_{BK}	- 3725 psi
ΔP_{OB}	- 128 psi
Estimated Reservoir Pressure	**= 13995 psi**

From the simulation results, it can be concluded that the criteria to determine whether the influx is stopped or not is crucial in the application of the proposed method during circulating responses. All the data to apply the method is available on well site, and the only value that needs to be estimated is the overbalance safety factor. Nevertheless, the example above proved that the safety margin (ΔP_{OB}) can be determined without difficulties with information available in the rig; ΔP_{OB} is assumed to be equal to the total casing pressure imposed on the well after a match between flow in and flow out is achieved; hence, the method can be used to approximate reservoir pressure when circulating responses are applied.

5.3.1.3 Simulation Summaries

Based on the results of 36 simulations, a sensitivity analysis was performed to evaluate the effectiveness of the method described on this chapter. The simulations emulated drilling operations when a non-circulating or a circulating response was applied. Two kick sizes and three different underbalance conditions were simulated to test the method.

The simulation data used to estimate formation pressure from circulating conditions are listed in Table 5.3. It should be noted that during these simulations the ΔP_{OB} was managed to be 100 psi. Also notice that the actual reservoir pressures set in the simulator for each scenario are shown in the fourth column of the table, and the estimated formation pressures are listed on the last column; comparison graphs between these two values are shown later in this section.

Table 5.3 Simulation data – formation pressure estimation

Well	Initial Response	UB	Actual Res. Pres (psi)	Pit Gain (bbl)	BHP_{BK} (psi)	DPP_{BK} (psi)	DPP_{AK} (psi)	Estimated Res. Pres (psi)
LSU #2	NCR	UB1	3096	2	2942	1610	1865	3097
		UB2	3525				2298	3530
		UB3	3790				2545	3777
		UB1	3096	20			1860	3092
		UB2	3525				2290	3522
		UB3	3790				2560	3792
	CR	UB1	3096	2	2942	1610	1853	3085
		UB2	3525				2284	3516
		UB3	3790				2565	3797
		UB1	3096	20			1855	3087
		UB2	3525				2288	3520
		UB3	3790				2565	3797
WELL X	NCR	UB1	10860	2	10706	2950	3200	10856
		UB2	11289				3642	11298
		UB3	11555				3880	11536
		UB1	10860	20			3200	10856
		UB2	11289				3610	11266
		UB3	11555				3870	11526
	CR	UB1	10860	2	10706	2950	3206	10862
		UB2	11289				3628	11284
		UB3	11555				3883	11539
		UB1	10860	20			3197	10853
		UB2	11289				3630	11286
		UB3	11555				3910	11566
WELL Y	NCR	UB1	13606	2	13557	3725	3875	13607
		UB2	14000				4256	13988
		UB3	14245				4480	14212
		UB1	13606	20			3878	13610
		UB2	14000				4250	13982
		UB3	14245				4510	14242
	CR	UB1	13606	2	13557	3725	3900	13632
		UB2	14000				4246	13978
		UB3	14245				4495	14227
		UB1	13606	20			3883	13615
		UB2	14000				4243	13975
		UB3	14245				4476	14208

Figure 5.3 illustrates the estimated error and difference between the actual reservoir pressure set in the simulator and the estimated reservoir pressure. The average absolute errors and differences for the simulations performed on each well are also shown in the graphs. The horizontal axis corresponds to the difference in psi, and the vertical axis refers to the simulation scenario; the errors (%) are shown beside each comparison.

It can be observed that the proposed method estimated the reservoir pressure within 40 psi, and the maximum errors were -0.36%, and +0.19% for all the scenarios. The average error was

±0.13%. Notice that the average error in the formation pressure estimates in LSU#2 was only 6 psi versus 11 psi in well X and 17 psi in well Y. However, because BHP in LSU#2 is less than the rest of the wells, 6 psi represents a higher error: 0.18%. These average errors are considered acceptable because they represent significantly less error than gauges, typically 1% of full scale, (e.g 5,000 to 15,000 psi) 50 to 150 psi for gauges, and mudscale (e.g 0.05 ppg of 10.0 ppg mud is 0.5%) used in real operations. Finally, it is shown that the proposed method estimates formation pressure within an acceptable range; furthermore it can be applied either during a circulating response or following a non-circulating response.

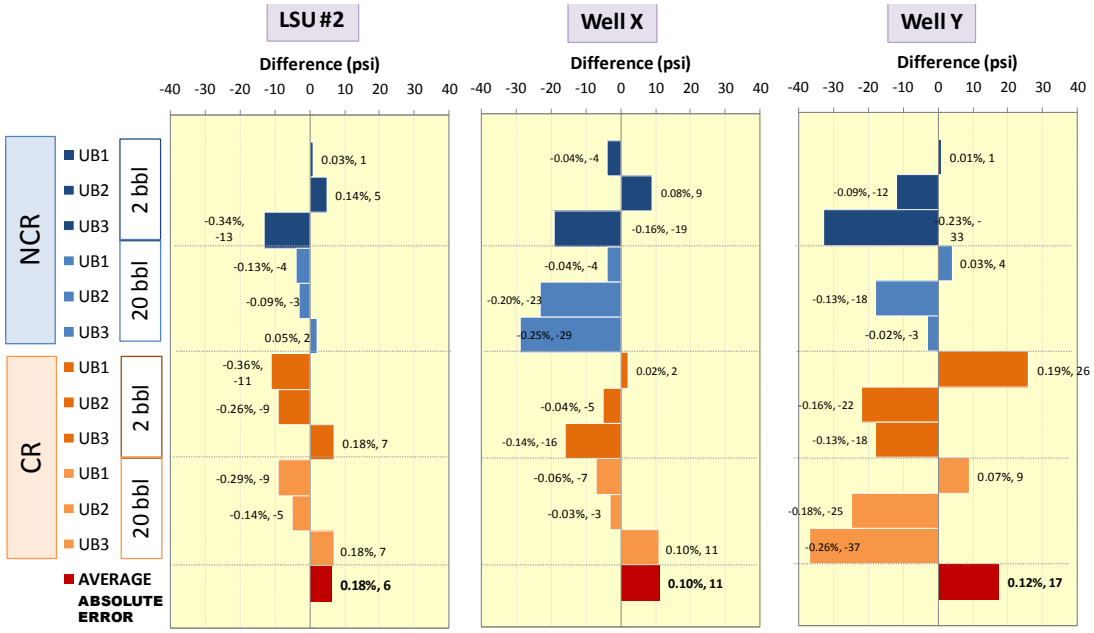

Figure 5.3 Comparison actual vs. estimated formation pressure (simulation results)

5.3.2 Full Scale Experiment

Full-scale test data was used to evaluate the proposed method. An apparent formation pressure was estimated for each of fifteen full scale experiments performed in 1986 (DEA Project 7) and one performed in 2009 by the MPD consortium using the procedure described in section 5.2. Data was recorded during the experiment, and the values needed to calculate the actual apparent formation pressure are shown in Table 5.4. BHP was determined by reading surface pressure in the injection

line and adding the hydrostatic pressure of the gas filling the tubing, and DPP was read from the pump gauge. It should be noted that on these experiments ΔP_{OB} was zero.

Table 5.4 Data full scale experiments

Test	SIDPP (psi)	MW (ppg)	BHP_{BK} (psi)	DPP_{BK} (psi)	DPP_{AK} (psi)
1-3	450	8.6	3034	950	975
1-4	450	8.55	3018	1050	1125
1-5	450	8.6	3029	950	970
2-2	585	8.75	3099	570	675
2-3	560	8.7	3154	1235	1300
2-4	600	8.7	3074	1215	1380
2-5	580	8.7	3184	1300	1355
3-2	450	12.5	4184	1180	1270
3-3	450	12.3	4114	1160	1225
3-4	450	12.4	4154	1260	1340
3-5	455	12.4	4114	1180	1250
4-2	430	12.35	4059	1150	1315
4-3	565	12.4	4159	1150	1330
4-4	600	12.3	4134	1160	1380
4-5	600	12.3	4134	1145	1400
MPD test	478	8.6	2868	1271	1478

Table 5.5 shows the estimate of apparent formation pressure using Eq. 5.4 for each test. The actual reservoir pressure was calculated by the conventional method discussed in section 2.3.4. The results were compared by estimating the percent error and the differences between actual and estimated apparent formation pressures. The results also are illustrated on Figure 5.4; it can be observed that the maximum difference between actual and the estimated reservoir pressure is 65 psi which represents a 1.48% error. This difference may be attributed to experimental conditions such as difference in accuracy between the drillpipe and injection line gauges or an error in the mud scale reading. Finally, from these experiments an average percent error and an average difference were estimated to be 0.70% and 26.6 psi respectively. These results give practical credibility to the proposed method and support the conclusion achieved with computer simulations.

Table 5.5 Apparent formation pressure results

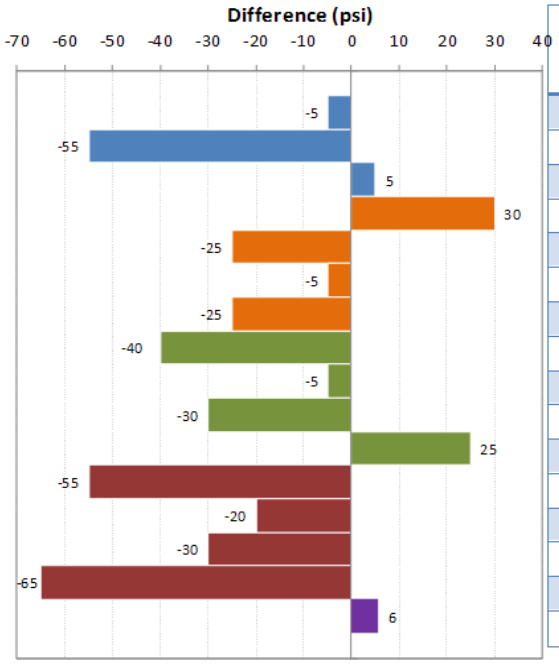

Tests	Estimated Res. Pres (psi)	Actual Res. P (psi)	Error (%)
1 -3	3059	3054	0.16%
1 -4	3093	3038	1.78%
1 -5	3049	3054	-0.16%
2 -2	3204	3234	-0.94%
2 -3	3219	3194	0.78%
2 -4	3239	3234	0.15%
2 -5	3239	3214	0.77%
3 -2	4274	4234	0.94%
3 -3	4179	4174	0.12%
3 -4	4234	4204	0.71%
3 -5	4184	4209	-0.60%
4 -2	4224	4169	1.30%
4 -3	4339	4319	0.46%
4 -4	4354	4324	0.69%
4 -5	4389	4324	1.48%
MPD test	3076	3082	-0.18%

Figure 5.4 Comparison between actual and estimated apparent formation pressure

5.4 Summary and Conclusions

The method described in this chapter proved to provide a reasonable approximation of the reservoir pressure for MPD well control operations. The elements needed to apply the procedure are generally available at the rig. Furthermore, the expression is very simple, and it only implies the addition and subtraction of four parameters: estimated or measured bottomhole pressure before the kick was taken (BHP_{BK}), drillpipe pressure after kick is controlled (DPP_{AK}), drillpipe pressure before kick (DPP_{BK}) and the safety overbalance (ΔP_{OB})

$$P_p = BHP_{BK} + DPP_{AK} - DPP_{BK} - \Delta P_{OB} \qquad \text{(Eq. 5.5)}$$

This expression was tested satisfactorily for simulated well control events where non-circulating and circulating responses were performed. Determination of the ΔP_{OB} is necessary when applying this expression: if a non-circulating response is applied, the ΔP_{OB} will depend on the

accurate interpretation of the stabilized SICP, the additional SICP ($=\Delta P_{OB}$) and the correct application of the pump start up after the shut in period. If a circulating response is applied, the ΔP_{OB} will rely on the correct selection of when the influx is stopped and the correct reading of the casing pressure imposed after the kick is controlled. The difference of these two values is the ΔP_{OB}. In either case, there is sufficient information on site to document the correct parameters and estimate the reservoir pressure with this method.

Finally, simulations and full scale experiments showed the application of this method during non-circulating and circulating responses gave reasonable and useable estimates of formation pressure. A sensitivity analysis revealed that the average difference between the actual reservoir pressure and the estimated formation pressure during the computer simulation and the full scale experiments were 11.3 psi (0.1%) and 26.6 psi (0.7%) respectively which are a reasonable approximation. This study demonstrated that this method can be used to approximate reservoir pressure during MPD well control operation.

Chapter 6 Casing Pressure in MPD Well Control

6.1 Introduction

The Constant Bottom Hole Pressure (CBHP) method of Managed Pressure Drilling (MPD) allows more precise control of wellbore pressure than conventional drilling. It also provides advantages for controlling kicks; one of them is the ability to perform well control operations by using the rotating control device (RCD) in place of the annular preventer. An important caveat is that the pressure rating of the RCD must exceed the maximum casing pressure experienced during kick circulation. This peak casing pressure is typically estimated by applying a single bubble calculation or using a computer simulation. However, single bubble calculations generally overestimate maximum casing pressure, and computer simulations are not always available, potentially resulting in overdesigned MPD equipment or operations. This chapter describes a new simplified method of graphs and calculations based on empirical data that allows prediction of maximum casing pressure during kick circulation, and it also demonstrates the use of the kick tolerance concept in conjunction with the new method in MPD well planning. Finally, a validation process based on full scale experiments and computer simulations is performed to support the application of the new method.

6.2 Maximum Casing Pressure

Depending on what type of initial response is applied to a well control event, the maximum casing pressure will occur at the beginning of the well control operation or during kick circulation. Figure 6.1 shows casing pressure variation in time during three well control operations simulated in well X. The simulations emulate well control operations when a 20 bbl kick enters well X with 0.2 ppge circulating underbalance. Two types of initial responses were applied: one circulating response (red line), and two non-circulating responses. When the non-circulating responses were applied, the kick

was circulated out one time with reduced rate (blue line) and one time with full rate (purple line). It can be seen in Figure 6.1 that during the circulating response, the maximum casing pressure occurs during kick circulation when most of the gas reaches surface. However, when a non-circulating response is applied for this example, peak casing pressure happens at the beginning of the well control event during the shut in period (full rate) or during kick circulation when most of the gas reaches surfaces (reduced rate).

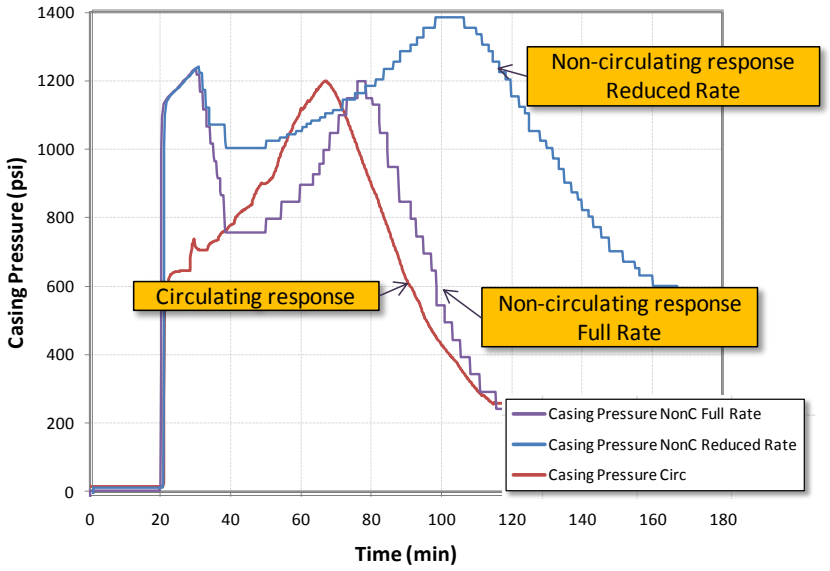

Figure 6.1 Maximum casing pressure in circulating and non-circulating responses

6.3 Maximum Casing Pressure Estimation

The evaluation of the casing variation during kick circulation started by developing a simplified method to estimate maximum casing pressure during kick circulation. The method is based on the gas law and empirical correlations for a triangular gas distribution published by Ohara in 1996 (section 2.3.3). The detailed procedure used to estimate maximum casing pressure during kick circulation is described as follows:

1. Determine the deepest depth (D_1) where gas velocity is greater than the mixture velocity. Using Ohara's empirical plots, the depth where the gas starts migrating and moving faster than the

mud can be determined by entering Figure 6.2 with the drilling fluid velocity and intercepting the front velocity line or by solving Eq. 2.15. During this step the gas is assumed to travel at the same velocity of the mixture until it reaches D_1.

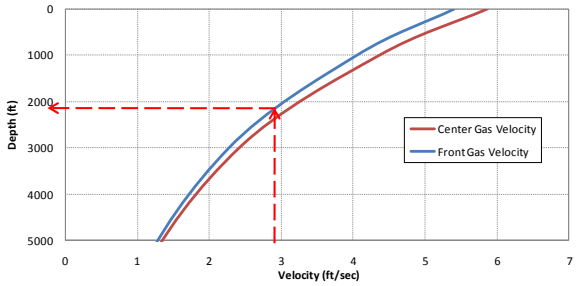

Figure 6.2 Empirical gas velocity (Ohara 1996)

2. Based on Ohara's experimental data, an average gas velocity plot and equations for the front and the center or apex corner of the triangular distribution was determined (Figure 6.3). The average velocities come from the gas velocities at depth above the depth of interest. Using this plot or equations Eq. 6.1 and Eq. 6.2, the average velocities (V_{front} and V_{apex}) from D_1 to the surface are estimated. It is assumed that the tail corner of the triangle travels at the same velocity of the liquid ($V_{tail} = V_{liquid}$).

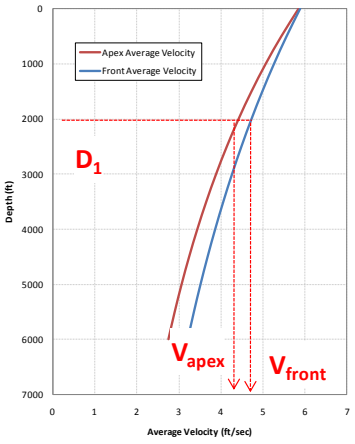

Figure 6.3 Average velocity front and apex

$$V_{front} = (3.132\ x\ 10^{-8})\ D_1^2 - (6.2854x10^{-4})\ D_1 + 5.8677 \qquad \text{(Eq. 6.1)}$$

$$V_{apex} = (4.6029\ x\ 10^{-8})\ D_1^2 - (7.8566^{-4})\ D_1 + 5.8246 \qquad \text{(Eq. 6.2)}$$

3. The pressure and volume of gas at depth D_1 are estimated by applying the single bubble method discussed in section 2.3.2.1. Applying equations Eq. 2.8 and 2.10, the initial pit gain is used to approximate pressure, volume and length of the gas at this depth (h_{D1}). It is assumed that the pressure is the same throughout the gas.

4. Given that this method is based on the assumption of a triangular gas distribution, the length of the base of the triangle (h_o) can be estimated by setting the area of the rectangular distribution of the single bubble method to the area of the triangular shape of this method (Figure 6.4). Notice that the single bubble method assumes a gas fraction (α) equal to 100%; however, this method assumes α = 66.66% as a maximum gas fraction at D_1 0. This assumption is based on empirical data from Ohara's research and data from DFD simulations. These two concepts are combined to derive the following equation:

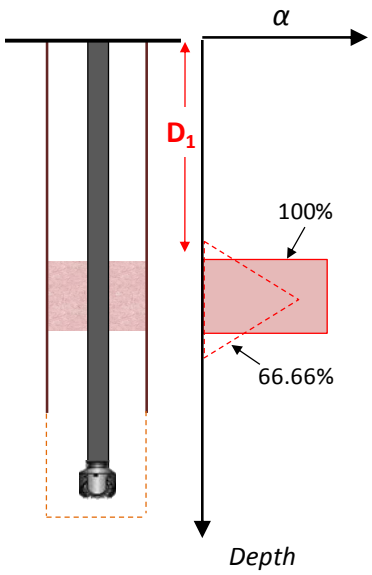

Figure 6.4 Triangular gas distribution

$$A_{rectagle} = A_{triangle}$$

$$\alpha_{(100\%)}\, h_{D1} = \frac{\alpha_{(66.66\%)}\, h_o}{2}$$

$$h_o = 3\, h_{D1} \qquad \text{(Eq. 6.3)}$$

5. Using the average velocity of the front corner of the triangle (V_{front}), the time required for the leading edge to reach the surface from D_1 estimated by applying the following equation:

$$t_{front} = \frac{D_1}{V_{front}} \qquad \text{(Eq. 6.4)}$$

6. The depths of the apex and the tail corners of the triangle when the gas first reaches surface are estimated using the average velocities and the time found in step 5. Notice that the length of the base of the triangle is equal to the depth of the tail corner at this moment.

$$D_{apex} = D_1 + \frac{h_o}{2} - \left(V_{apex}\ t_{front}\right) \qquad \text{(Eq. 6.5)}$$

$$D_{tail} = D_1 + h_0 - \left(V_{tail}\ t_{front}\right) \qquad \text{(Eq. 6.6)}$$

7. The gas volume ($V_{D\ apex}$) is estimated at depth D_{apex} applying gas law using equations Eq. 2.8 and 2.10.

8. Gas volume, annular area and depth of the tail corner are used to estimate the average gas fraction of the gas inside the well:

$$\alpha_{average} = \frac{V_{D\ apex}}{A_{an} D_{tail}}\ or\ \frac{h_{gas}@\ D_{apex}}{D_{tail}} \qquad \text{(Eq. 6.7)}$$

9. Using a similar approach in step 4, the maximum gas fraction is estimated relating the areas of the rectangle and the triangle shown in Figure 6.5.

$$A_{rectangle} = A_{triangle}$$

$$\alpha_{max} = 2\ \alpha_{average} \qquad \text{(Eq. 6.8)}$$

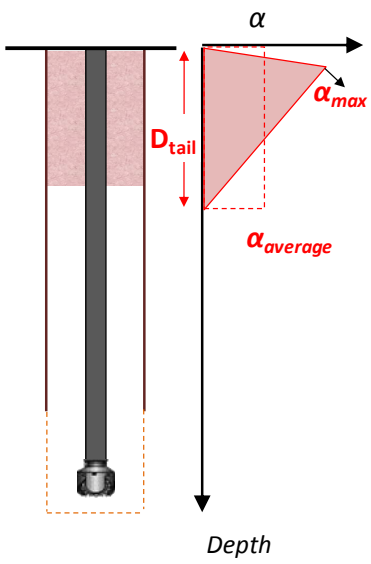

Figure 6.5 Gas fraction relation

10. The equivalent h2ydrostatic loss (ΔP_{hyd}) when the apex corner reaches the surface is then estimated as:

$$\Delta P_{hyd} = 0.052\ EMW \frac{\left[\left(D_{tail} - D_{apex}\right)\alpha_{max}\right]}{2} - P_{hg} \qquad \text{(Eq. 6.9)}$$

11. Finally, the maximun casing pressure during kick circulation is assumed to occur when the maximum gas fraction reaches the surface and is estimated as follows:

$$CP_{max} = \Delta P_{hyd} + \Delta P_{UB} \quad \text{(Eq. 6.10)}$$

After this method was defined, a broad range of simulations and full scale experiments were used to study the casing pressure behavior during kick circulation. An example calculation for well X is provided in Appendix B. This method was applied in the different scenarios, and it was compared with single bubble calculations, simulations and actual casing pressures from full-scale well experiments.

6.4 Simulation Results

A broad range of simulations were performed to compare the maximum casing pressure during circulation to the casing pressure estimated with the new method. This section shows and discusses the application of the proposed method in full scale experiments and in computer simulations.

6.4.1 Full Scale Experiments

Comparison of the proposed method was made to full scale experimental data described in section 3.4.1. This data contains 15 full kick circulations under different conditions. Four drilling fluid rheologies, pump rates between 90 and 133 gpm, initial underbalance between 300 and 500 psi, and kick sizes between 9 and 11 bbl were some of the variations (refer to Table 3.1 for more details). Finally, single bubble calculations and computer simulations were performed for each test to compare and validate the application of the proposed method.

Figure 6.6 compares the actual maximum casing pressure to the estimates by the three methods: single bubble, computer simulation and the proposed method. On the graph, the horizontal axis corresponds to the 15 full scale experiments, and the vertical axis shows the maximum casing pressure during circulation (CP_{max}). The purple line represents the actual CP_{max} read

from the experimental data. It can be observed that single bubble estimations (blue line) over predicted CP_{max} by an average of ±200 psi; this performance was expected because this technique is based on oversimplified and incorrect assumptions. The computer simulation results (orange line) gave a better estimation of CP_{max} than the single bubble technique; however, in this particular case, it can be seen that it overestimates CP_{max} by an average of ±80 psi. Although it is clear that Dynaflowdrill™ over predicts CP_{max} on these experiments, this performance cannot be generalized to all well geometries and all depths. Finally, a red line represents CP_{max} estimated by the proposed method. It is shown that the proposed method achieved good agreement with the actual CP_{max} in all experiments. The average differences between the actual and the estimated CP_{max} were only 26.6 psi or 3.99%.

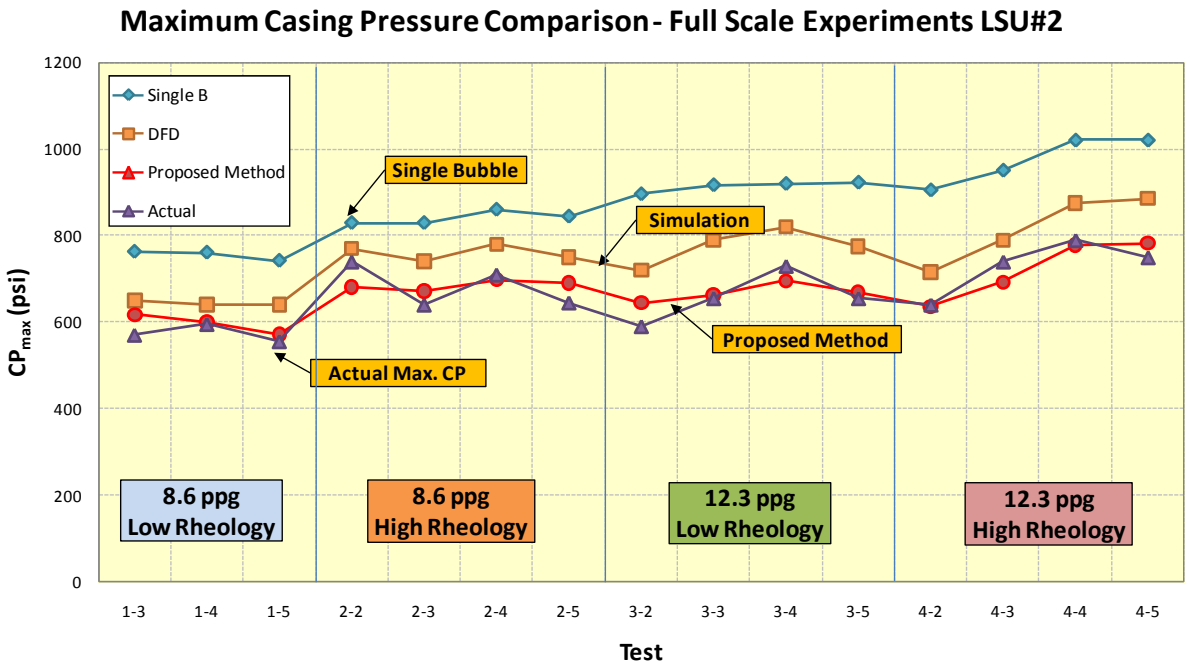

Figure 6.6 Peak CP comparison actual/single bubble/simulations/proposed method

Figure 6.7 shows difference in percentage and pressure between estimated and actual CP_{max} for each test. It is the relation between the proposed method CP_{max} and the actual CP_{max}. It is shown that CP_{max} was estimated within 10% and 60 psi of the actual peak casing pressure; these estimations are good enough to confirm the application of this method to approximate circulating pressure in a

well control event, at least for this hole size, kick volumes and range of pump rates. For the LSU#2 well geometry, the proposed method gave a consistently more accurate estimate of peak casing pressure than either a single bubble calculation or DFD simulation. However, it should be noted that this well geometry is the same well geometry used by Ohara in 1996 during his experiments on distribution; therefore, it is not possible to conclude that the method will have the same performance in all operational conditions. Consequentially, it is recommended this method be used only as an indicator until further evaluation with a wider range of real data can be performed. A limited effort to act on this recommendation is reported in Appendix C. Comparison with a full scale experiments performed in 1972 in a previous LSU well is given. It shows that after applying a small safety factor proposed later in this chapter the predictions were within 60 psi and 6% of actual pressures

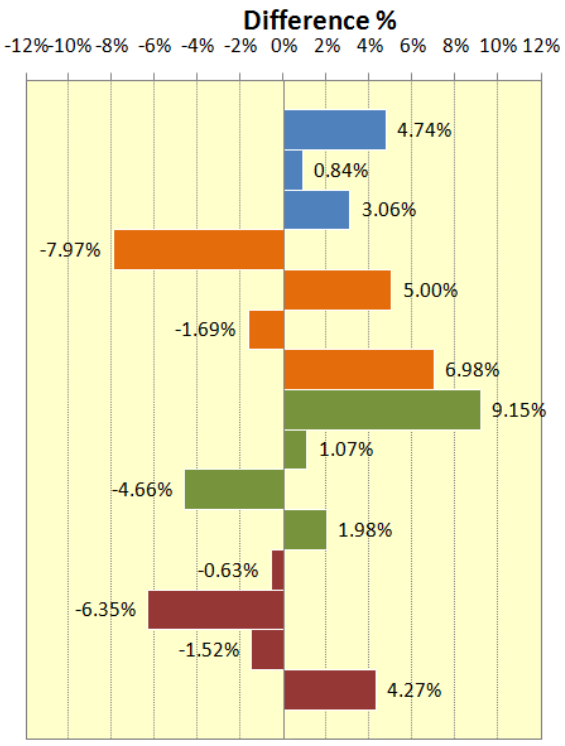

Test	Actual (psi)	Proposed Method (psi)	Difference (psi)
1 -3	570	597	27
1 -4	595	600	5
1 -5	555	572	17
2 -2	740	681	-59
2 -3	640	672	32
2 -4	710	698	-12
2 -5	645	690	45
3 -2	590	644	54
3 -3	655	662	7
3 -4	730	696	-34
3 -5	655	668	13
4 -2	640	636	-4
4 -3	740	693	-47
4 -4	790	778	-12
4 -5	750	782	32

Figure 6.7 Error analysis full scale experiences

6.4.2 Computer Simulations

Computer simulations were used for a larger variety of well geometries and kick conditions to allow more general evaluation of the proposed method. In order to be consistent with what is discussed in section 3.4.2, three well geometries were simulated in Dynaflowdrill™ under different operational conditions; eight scenarios for each well are presented in this section in which CP_{max} was computed using the method described in section 6.3 to compare to the proposed method. Single bubble estimations were also performed for comparison of all three techniques.

Figure 6.8 illustrates CP_{max} comparisons for the three well geometries. The graphs on the left column show the CP_{max} relationship between simulations and estimations with the proposed method. The red solid lines correspond to the best linear fit to the relationship between the two techniques, and the green dashed lines represent a reference of the ideal ratio between the CP_{max} evaluations. The plots on the right column give comparisons between CP_{max} estimated by the three techniques: simulation (purple line), single bubble (blue line) and the proposed method (red line); the vertical axis shows the CP_{max} estimated, and the horizontal axis indicates the specific test conditions.

The first two graphs refer to the simulations run for LSU #2. On the left graph it can be seen that the linear fit of the relationship between the simulated and calculated CP_{max} is close to ideal. However, when the plot on the left is observed, differences between simulations and the proposed method estimations are visible. During these simulations, the maximum difference in pressure was 111 psi or 9.79%; yet, the maximum percentage difference was 11.25% which corresponds to an 88 psi difference; these scenarios correspond to a 20 bbl pit gain with an initial underbalance of 0.5 ppge and 1.9 ppge respectively. The average difference for this well geometry was 7.04% and the average difference was 67 psi; both represent a reasonably approximation to the simulation results. Alternatively, single bubble estimations over predicted CP_{max} based on the simulation by an average of 80.9 psi and 8.97% $CP_{max.}$.

Well X, characterized by a slim hole geometry, is the second well shown in Figure 6.8. The left graph shows that the relationship between the simulations, and the proposed method is not as close as it is in the well LSU #2. However, if the plot on the right is observed, it is possible to distinguish that the proposed method gave similar estimates for the 2 and 10 bbl scenarios. The approximations of CP_{max} for these cases were within 100 psi of the simulation results, which is considered very good. Conversely, the proposed method did not compare well in the 20 bbl kick scenarios; the average difference on these tests was 272 psi. Although the performance was unfortunate for the 20 bbl kick scenarios, the general averages for the eight scenarios were 140 psi and 13.7% which represents an acceptable approximation. In addition to this information, the graph also shows that single bubble technique did not perform well under these operational conditions; it over predicted CP_{max} by an average of approximately 650 psi.

The third well shown in Figure 6.8 is well Y. It can be observed from the two graphs that the proposed method compared very well with the predicted CP_{max} throughout all the simulations. The maximum differences during these simulations were 74 psi and 14.68%, and the average differences were only 33 psi and 5.33% which are considered good. Alternatively, single bubble estimations were high all the time; the minimum was 100 psi and the maximum was 580 psi.

From the Figure 6.8, it can be concluded that the proposed method of approximating the maximum casing pressure during circulation corresponds relatively well to simulation results. However, comparisons indicate that 20 bbl kicks and slim hole geometries tend to decrease the agreement between the new method and the simulation results. Section 6.4.3 analyses results from these simulations and discusses possible approach to solve this problem.

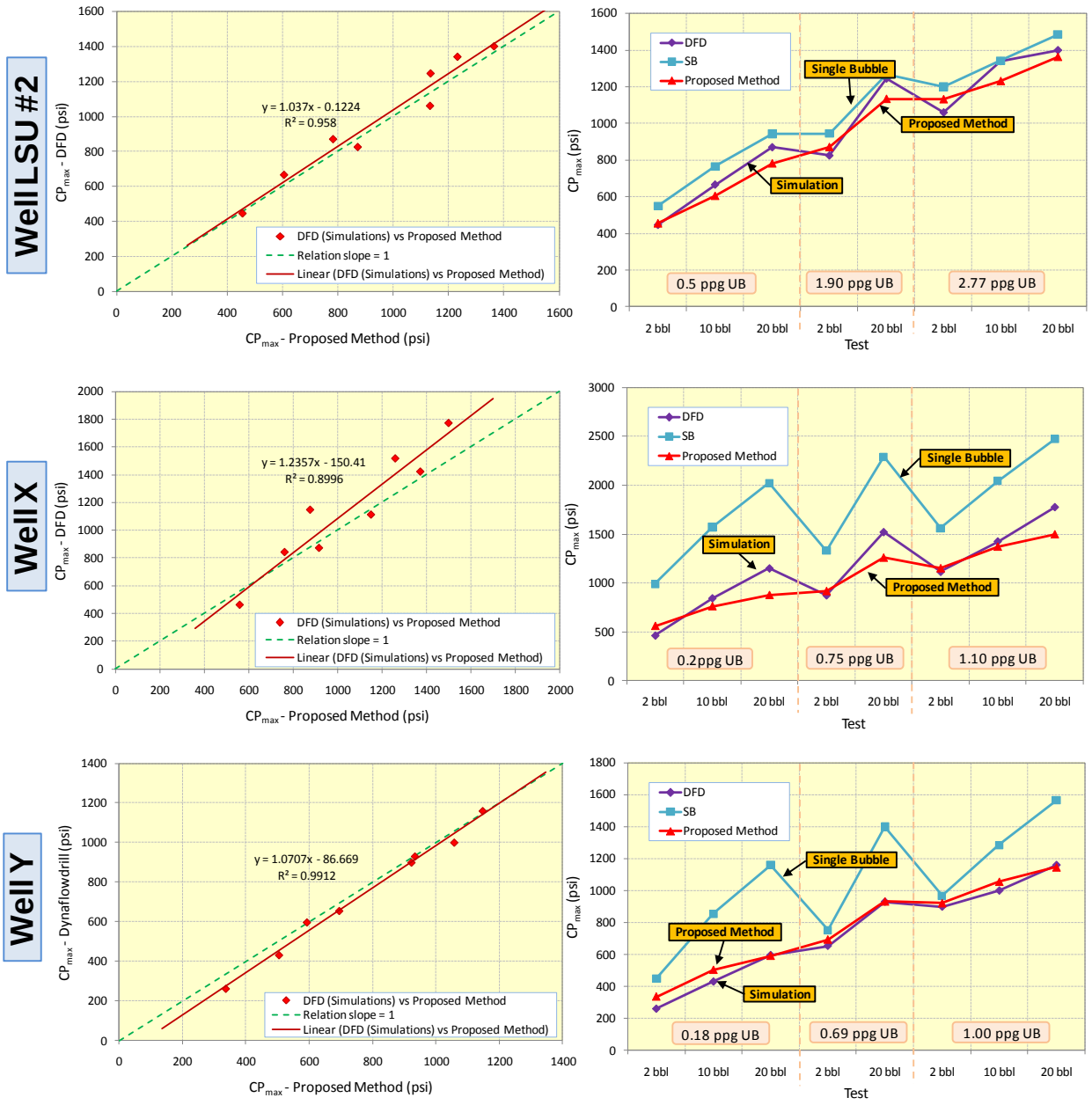

Figure 6.8 Comparison simulation vs. single bubble vs. proposed method

6.4.3 Analysis of Results

The results from computer simulations and full scale experiments indicate that the new method can be used to estimate maximum casing pressure during kick circulations. However, additional consideration is appropriate before the method is applied in well planning and well control events.

Figure 6.9 illustrates the difference in pressure for the tests performed in this research. Tests are categorized by pit gain sizes and type of data: simulated and experimental.

Full scale experiments provide a desirable source of validation; the results from these were approximated by computer simulations and the proposed method. The graph (Figure 6.9) on the right shows the full scale experiment results. It provides evidence that the proposed method predicted CP_{max} within 60 psi, which is a very good. However, this performance cannot be extrapolated to all well configurations or kick sizes, and more real data is needed to generalize its application.

On the left side of Figure 6.9, simulation results are plotted. This graph shows that the proposed method underestimated CP_{max} versus most of the 20 bbl simulation cases, and the comparison was worst in Well X. Also, it can be observed that the 10 bbl simulations were under predicted by an average 72 psi. Conversely, 2 bbl kick simulations were overestimated by an average of 44 psi for all the well geometries. In general this approximation are good; nevertheless, it should be noted that the comparisons are being made with the commercial simulator Dynaflowdrill™, and it is assumed that this computer program provides good assessment of the casing pressure during well control operations.

Application of a safety factor is recommended when the proposed method is being used. Table 6.1 shows the proposed safety factor to apply to the CPmax estimated with the proposed method. The values of the safety factors are based on the performance of the method under different conditions, and they intent to keep the CP_{max} over the simulation result.

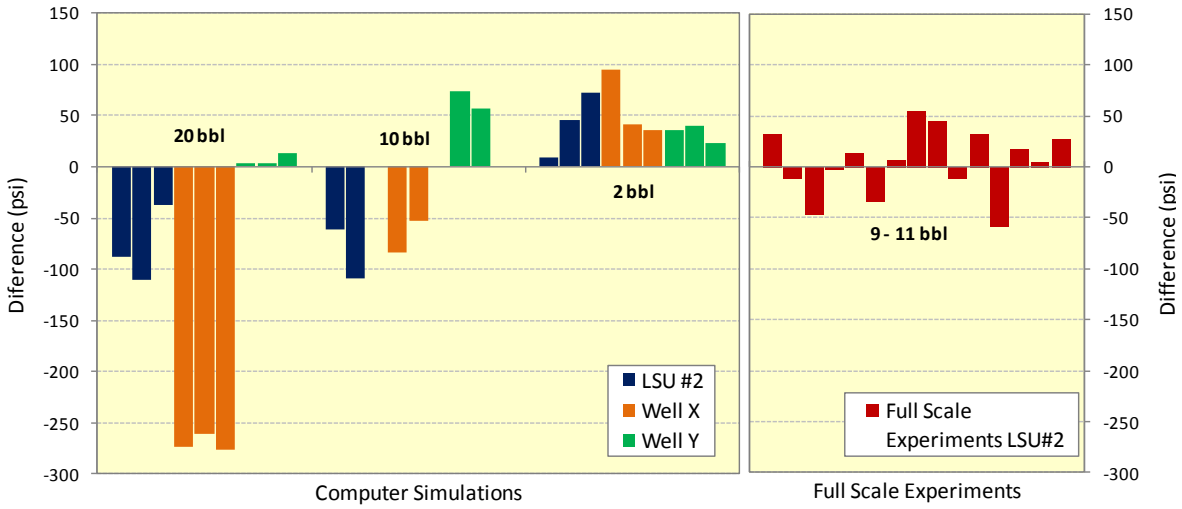

Figure 6.9 Pressure difference in simulations

Table 6.1 Safety factor recommended

Kick Sizes (bbl)	Safety Factor
1 – 5	1.05
5 – 15	1.1
15 above	1.2

6.5 Applications

The proposed method is intended to be used during both well planning and well control situations. Part of the well planning process includes the assessment of a well design to meet the desired operational limits. One limit is the desired kick tolerance to be achieved with expected formation strength and surface equipment. This section shows an example of the application of the new method when applying the kick tolerance concept in well planning.

Assume that well Y is in the planning phase, and that a comparison of the operational limits of the well and equipment to the desired kick tolerance is needed to complete the drilling planning. The initial surface pressure during a possible well control event can be estimated applying the kick

tolerance concept. Depending on what kind of initial response will be applied, the initial casing pressure after a kick (CP_{AK}) can be approximated as follow:

Non-circulating responses $$CP_{AK} = CP_{BK} + Circ\ UB + \Delta P_{KD} + \Delta P_{AF} + \Delta P_{OB}$$ (Eq. 6.11)

Circulating responses $$CP_{AK} = CP_{BK} + Circ\ UB + \Delta P_{KD} + \Delta P_{OB}$$ (Eq. 6.12)

Where CPBK = casing pressure during routine operations (psi); Circ UB = circulating underbalance (psi) assumed when worst case kick is taken; ΔPKD = loss of hydrostatic pressure due to the worst case volume and density of kick influx (psi); ΔPAF = annular frictional pressure loss (psi) during routine circulation; and ΔPOB = desired overbalance (psi) during kick circulation. Notice that the only difference between these two expressions is the addition of ΔPAF to the non-circulating response equation. This is because during circulating response the friction of the well is used help to control the kick, and therefore the casing pressure is less (refer to section 2.2.3).

A plot can be prepared to allow a general assessment of a well design kick tolerance. In this example, it has been decided to apply a circulating response if a well control event occurs. Figure 6.10 was prepared for well Y using 2 and 20 bbl kick volumes as representive of kick detection limits and a range of circulating underbalance from 0.2 to 1.0 ppg

Notice that Figure 6.10 illustrates examples of boundaries that need to be considered in MPD well planning (dashed red lines): (1) the maximum allowable surface pressure (MAASP) while circulating and (2) the rotating control device (RCD) pressure rating used in MPD operations. From the graph it can be inferred that if a 20 bbl kick is taken the maximum underbalance allowed at the initial response is 0.54 ppge. Alternatively, if a 2 bbl kick is taken the maximum underbalance allowed increases to 0.72 ppge. Nevertheless, Figure 6.10 was built with information at the beginning of the well control event, and it is still unclear if the maximum casing pressure will occur initially or during kick circulation. Using the proposed method, a new plot (Figure 6.11) with the

maximum casing pressure during kick circulation can be built to compare and decide which casing pressure should be used in well planning.

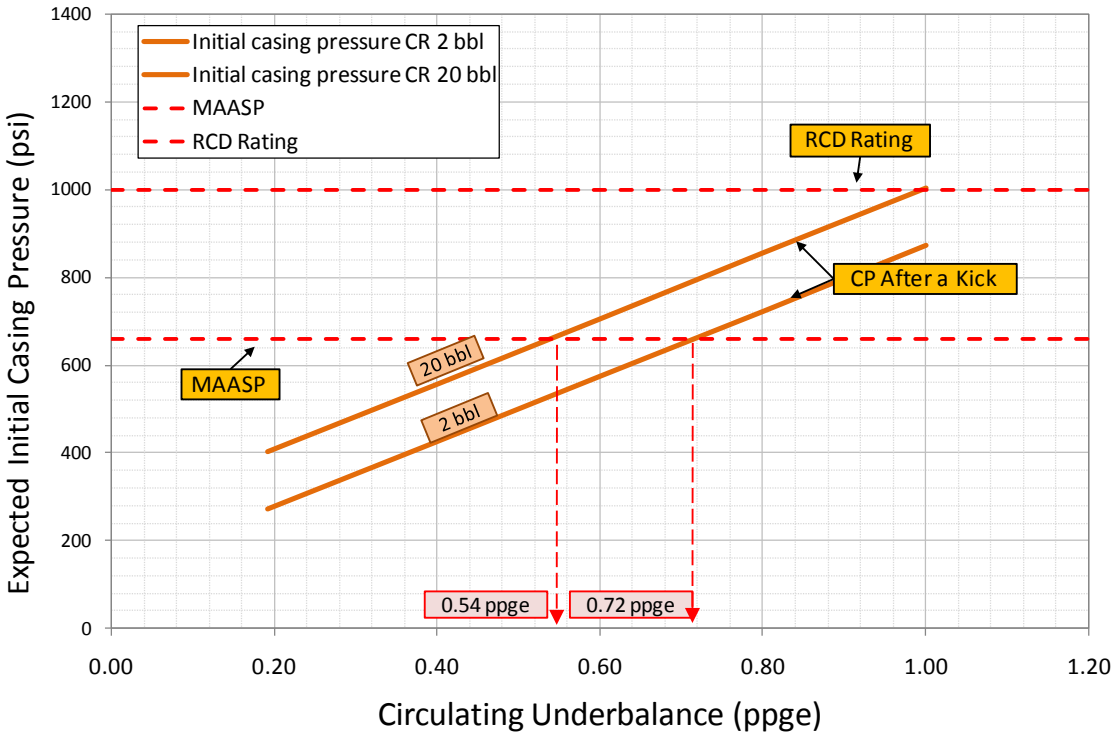

Figure 6.10 Expected initial casing pressure after circulating responses for well Y

Figure 6.11 reveals that for this case the casing pressures are going to be higher during kick circulation than at the beginning of the well control operation; therefore, the two blue lines representing the circulating casing pressure must be used in well planning instead of the casing pressure at the beginning of operation (yellow line). Another implication of the chart is that the limits on circulating underbalanced mentioned before are confirmed to be inside the RCD rating, and therefore the expected casing pressure during circulation will not jeopardize the integrity of the operation. For example, it can be read that the maximum circulating underbalance allowed by the RCD rating with 20 and 2 bbl initial kick sizes are 0.76 and 1.10 ppge, respectively. The RCD rating limitation does not affect the initial integrity boundaries found in Figure 6.10 (0.54 ppge 2 bbl and 0.72 ppge 20 bbl) because they are outside the initial integrity boundaries of operations. Consequently, this approach reveals true boundaries that were not clear at first glance, and its

application increases awareness of the limits of the operations. This information may lead the engineer to improve the kick detection methods used to reduce the pit gain anticipated before initiating a response in well control scenarios, or modified rig equipment such as an RCD with higher pressure rating if it is necessary. Finally, the combination of the new method and the concept of kick tolerance can be very beneficial to well planning, and it definitely should be used to asses realistic boundaries for planned drilling operations.

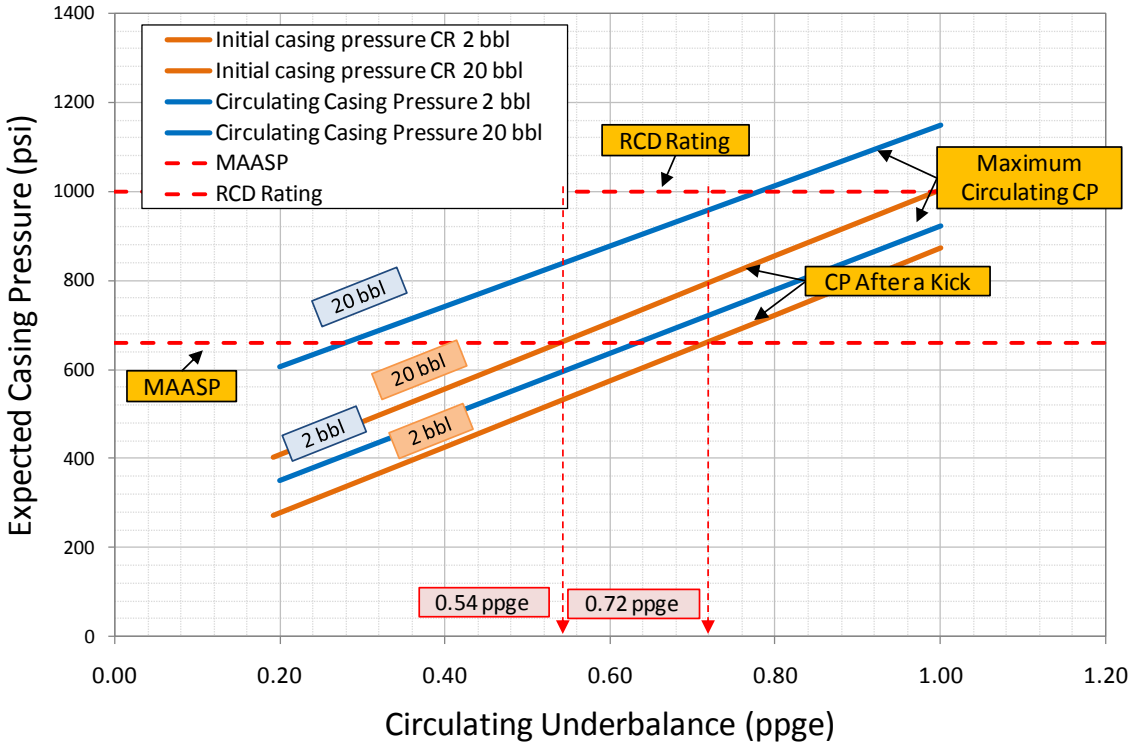

Figure 6.11 Expected maximum casing pressure for well Y

6.6 Summary and Conclusions

The proposed method discussed in this chapter proved to be able to approximate maximum casing pressure (CP_{max}) during kick circulation with relatively good accuracy. The method relies on the application of hydrostatic pressure and gas law calculations, and it includes empirical information related to gas distribution in kick circulation published by Ohara in 1996. This model can easily be programmed in an Excel spread sheet and used during MPD well planning or well control.

The model was tested against full scale experiments and computer simulations. Full scale experimental data reveals that the proposed method was able to give good approximation by estimating CP_{max} within 60 psi or 3.99%. The proposed method gave a consistently more accurate estimate of peak casing pressure than either a single bubble calculation or DFD simulation. Alternatively, a simulation study was carried out to evaluate the proposed method. It revealed a significant difference in predictions between these two methods in a slim hole well with 20 bbl pit gain; however, the rest of the CP_{max} with the new method destimates achieved a relatively good agreement with the computer simulations. Consequently, this method is intended to be used as a boundary indicator. More real data in different well geometries and operational conditions is needed to complete a comprehensive assessment of the model. Section 6.4.3 recommended safety factors to be used to offset potential error when this method is applied.

Finally, this method can be combined with the kick tolerance concept to evaluate operating boundaries during MPD operations. The example in section 6.5 illustrates the importance of knowing CP_{max} for well planning. It was shown that the casing pressure during kick circulation may exceed initial casing pressure in well control operations, and it needs to be determined to evaluate whether the equipment and design of a particular well will provide the desired kick tolerance, or conversely, what the allowable kick size and circulating underbalance will be with the planned well design and equipment.

Chapter 7 Conclusions and Recommendations

A university-industry consortium has studied alternative well control procedures to be used in kicks taken during managed pressure drilling (MPD) operations using the constant bottomhole pressure (CBHP) method. The CBHP method allows more precise control of wellbore pressure than conventional method; nevertheless, some considerations must be made during well control operations and well planning to be able to take full advantage of the CBHP method. In this research, computer simulations were used for comparison to a range of realistic well conditions. Full-scale gas kicks experiments were done to confirm applicability to a limited range of real situations. Three areas were studied: pump start up after a non-circulating response, formation pressure determination during CBHP well control operations and casing pressure prediction during kick circulation. Conclusions for each area are summarized in this section.

7.1 Conclusions

7.1.1 Pump Start up Method for Kick Circulation

1. The pump start up method described in Chapter 4 confirmed to minimize bottomhole pressure (BHP) fluctuation to ± 50 psi during pump start up.
    a. It is applicable after all non-circulating responses.
    b. It is based on the pump start up schedule for routine operation, which is very convenient.
2. The selection of the kick circulating rate after a non-circulating response must be based on equipment and formation limitations.
    a. Full circulating rate would require higher pump pressure and more separation capacity.
    b. Reduced pump rate would produce higher casing pressure.

3. Achieving the desired overbalance (ΔP_{OB}) during kick circulation would depend on three factors:
    a. The correct interpretation of the shut in casing pressure (SICP).
    b. The effect of annular space changes related to BHA component during kick circulation.
    c. Necessary pressure fluctuation during choke manipulation.

7.1.2 Formation Pressure in MPD operations

1. The method presented to evaluate reservoir pressure based on circulating pressures shown to give reasonable and useable estimates of formation pressure. The maximum errors were 0.1% and 0.7% for computer simulations and full scale experiments respectively.
2. The safety overbalance factor (ΔP_{OB}) that is being used must be known to obtain a valid approximation of formation pressure.
    a. During non-circulating responses, ΔP_{OB} depends on the correct interpretation of SICP.
    b. During circulating responses, ΔP_{OB} relies on knowing the additional casing pressure imposed after the kick is controlled.

7.1.3 Casing Pressure in MPD Well Control

1. Maximum casing pressure (CP_{max}) after a circulating initial response occurs during kick circulation.
2. During non-circulating responses, CP_{max} can happen at beginning of the event or while the kick is being circulated.
3. The proposed simplified method to estimate CP_{max} during MPD well control approximates maximum pressure with relatively good accuracy, within an average of 3.99% and a

maximum error of 9.15% for full scale experiments in the LSU#2 well with a large range of fluid properties.

4. Computer simulations revealed differences in CP_{max} prediction between methods. However, the average difference between simulation results and the proposed method was 9.33%. The maximum error was 26.6% for the simulations done with well X.
5. The accuracy of this method to other hole geometries, annular velocity, and kick sizes is less certain. Therefore, a safety factor should be applied when the proposed method is used. Suggested safety factors are given in Table 6.1.
6. A single bubble calculation generally overestimates CP_{max}, and commercial simulators also often over predicted $CP_{max.}$ for actual full scale kick circulation experiments.
7. The combination of the kick tolerance concept and the proposed method demonstrated to reveal true boundaries related to operational limits in MPD operations. These limitations are related to surface equipment and formation strength.
    a. Kick tolerance can be estimated by assuming a kick size volume based on the expected kick detection sensitivity, and defining the kick intensity, i.e. possible underbalance due to uncertainty in pore pressure.

7.2 Recommendations

1. Although the methods proposed in this research have been simulated and tested versus full scale experiments and computer simulations, further full-scale tests or field experiences in different well geometries should be used to evaluate and reinforce the conclusions reached in this research.
2. More computer simulations should be used to identify possible drawbacks of the methods discussed in this research. Although three well geometries were simulated in this project, it is

recommended to expand the number of well geometries to study possible boundaries in the application of the methods proposed.

3. Modify the proposed methods to apply them to kicks taken off bottom, or develop a new approach to evaluate kick circulation under this condition.
4. Additional research related to gas distribution in kick circulation should be performed to reinforce the triangular distribution idea. Full scale data should be acquired from different well geometries and operational conditions, especially kick size and mixture velocity, to validate application of Ohara's empirical equations to all well scenarios or to create a database or a more generally applicable model of gas velocities.
5. Investigate possible improvements in the maximum casing pressure method discussed in Chapter 6:
    a. Estimate the average pressure of the gas inside the well when the maximum casing pressure is occurring. The method proposed assumed average pressure to be equal to the pressure on the top of the gas inside the well.
    b. Use mass or mole information to track gas volume during kick circulation.
    c. Investigate the assumed correspondence between actual peak casing pressure and peak gas concentration at the surface.
6. Investigate kick circulation in well control operations with lost returns, and develop a method to indentify this problem during kick circulation.

References

Arnone, M. A., and Vieira, P. 2009. "Drilling Wells With Narrow Operating Windows Applying the MPD Constant Bottom Hole Pressure Technology—How Much the Temperature and Pressure Affects the Operation's Design". Paper SPE/IADC 119882 presented at the SPE/IADC Drilling Conference and Exhibition, Amsterdam, The Netherlands, 03/17/2009. doi: 10.2118/119882-MS.

Bourgoyne, A. T. 1991. *Applied drilling engineering, SPE Textbook Series*. Dallas, Tex.: Society of Petroleum Engineering of AIME.

Calderoni, A., Chiura, A., Valente, P., Soliman, F., Squintani, E., Vogel, R. Elliot, and Jenner, J.W. 2006. "Balanced Pressure Drilling With Continuous Circulation Using Jointed Drillpipe - Case History, Port Fouad Marine Deep 1, Exploration Well Offshore Egypt". Paper SPE 102859-MS presented at the SPE Annual Technical Conference and Exhibition, San Antonio, Texas, USA. doi: 10.2118/102859-MS.

Das, A. K., Smith, J. R., and Frink, P. J. 2008. "Simulations Comparing Different Initial Responses to Kicks Taken During Managed Pressure Drilling". Paper IADC/SPE 112761-MS presented at the IADC/SPE Drilling Conference, Orlando, Florida, USA, 03/04/2008. doi: 10.2118/112761-MS.

Das, Asis Kumar. 2007. *Simulation study evaluating alternative initial responses to formation fluid influx during managed pressure drilling*. MS Thesis, Craft & Hawkins Department of Petroleum Engineering, Louisiana State University, Baton Rouge, LA.

Davoudi, M., Smith, J. R., Patel, B. M., and Chirinos, J.E. 2010. "Evaluation of Alternative Initial Responses to Kicks Taken during Managed Pressure Drilling". Paper IADC/SPE 128424 presented at the IADC/SPE Drilling Conference and Exhibition, New Orleans, LA, USA, 2-4 February. doi: 10.2118/128424-MS.

Davoudi, Majid. 2009. *A Simulation-based evaluation of Alternative Initial Responses to Gas Kicks During Managed Pressure Drilling Operations*. MS Thesis, Craft & Hawkins Department of Petroleum Engineering, Louisiana State University, Baton Rouge.

Dedenuola, A. D., Iyamu, I. E., and Adeleye, O. A. 2003. "Stochastic Approach to Kick Tolerance Determination in Risk Based Designs". Paper SPE 84174-MS presented at the SPE Annual Technical Conference and Exhibition, Denver, Colorado, 10/05/2003. doi: 10.2118/84174-MS.

EIA, Energy Information Administration. 2009. *Recent Petroleum and Natural Gas Consumption* 2009. Available on http://www.eia.gov.

Grayson, Michael B. 2009. "Increased Operational Safety and Efficiency With Managed Pressure Drilling". Paper SPE 120982 presented at the SPE Americas E&P Environmental and Safety Conference, San Antonio, Texas, 03/23/2009. doi: 10.2118/120982-MS.

Guner, H. 2009. *Simulation Study of Emerging Well Control Methods from Influxes Caused by Bottomhole Pressure Fluctuation during Managed Pressure Drilling.* MS Thesis, Craft & Hawkins Department of Petroleum Engineering, Louisiana State University, Baton Rouge.

Hannegan, Don M. 2006. "Case Studies--Offshore Managed Pressure Drilling". Paper SPE 101855 presented at the SPE Annual Technical Conference and Exhibition, San Antonio, Texas, USA. doi: 10.2118/101855-MS.

IADC. 2009. *Glossary of MPD and UBD* 2009. Available on http://www.iadc.org.

Jenner, J. W., Elkins, H., Springett, F., Lurie, P., and Wellings, J. S. 2005. The Continuous Circulation System: An Advance in Constant Pressure Drilling. *SPE Drilling & Completion* 20 (3):168-178.SPE 90702-PA. doi: 10.2118/90702-pa

Lima, J., and Pals, F. 2009. BP's Tiber Find Underscores Challenges of Deepwater Exploration. *Bloomberg.com*, http://www.bloomberg.com/apps/news?pid=20601109&sid=ak0cLK9YuS1E.

Malloy, K. P., Stone, R., Medley, G. Harold, Hannegan, D. M., Coker, Ol. D., Reitsma, D., Santos, H., Kinder, J., Eck-Olsen, J., McCaskill, J. Walton, May, J., Smith, K. L, and Sonnemann, P. 2009. "Managed-Pressure Drilling: What It Is and What It Is Not". Paper IADC/SPE 12228 presented at the IADC/SPE Managed Pressure Drilling and Underbalanced Operations Conference & Exhibition, San Antonio, Texas, 02/12/2009. doi: 10.2118/122281-MS.

Malloy, Kenneth P. 2008. A Probabilistic Approach to Risk Assessment of Managed Pressure Drilling in Offshore Applications. Joint Industry Project DEA155: U.S Department of the Interior Minerals Management Service.

Medley, G., Moore, D., and Nauduri, A.S. 2008. "Simplifying MPD - Lessons Learned". Paper SPE/IADC 113689-MS presented at the SPE/IADC Managed Pressure Drilling and Underbalanced Operations Conference and Exhibition, Abu Dhabi, UAE, 01/28/2008. doi: 10.2118/113689-MS.

MMS. 2008. Managed Pressure Drilling Projects. Gulf Of Mexico Ocs Region: US DOI.

MMS, Mineral Management Service. *Offshore Statistics by Water Depth Database* 2009. Available on http://www.gomr.mms.gov.

Nauduri, A., Medley, G., and Schubert, J. 2009. "MPD: Beyond Narrow Pressure Windows". Paper SPE/IADC 122276-MS presented at the IADC/SPE Managed Pressure Drilling and Underbalanced Operations Conference & Exhibition, San Antonio, Texas, 02/12/2009 doi: 10.2118/122276-MS.

Ohara, Shiniti. 1996. *Improved method for selecting kick tolerance during deepwater drilling operations*. PhD Dissertation, Craft & Hawkins Department of Petroleum Engineering, Louisiana State University Baton Rouge.

PERTT-LSU. Well Control Manual. Baton Rouge: Petroleum Engineering Research and Technology Transfer Laboratory - Louisiana State University.

Redmann Jr., K.P. 1991. Understanding Kick Tolerance and Its Significance in Drilling Planning and Execution. *SPE Drilling Engineering* 6 (4):245-249.SPE 19991-PA. doi: 10.2118/19991-pa

Rehm, Bill. 2009. *Managed pressure drilling*, *Gulf drilling series*. Houston, TX: Gulf Pub.

Reitsma, D. 2005. "Development and Application of Combining a Real-Time Hydraulics Model and Automated Choke To Maintain a Relatively Constant Bottomhole Pressure While Drilling". Paper IPTC 10708-MS presented at the International Petroleum Technology Conference, Doha, Qatar, 11/21/2005. doi: 10.2523/10708-MS.

Reitsma, D., and Riet, E. van. 2005. "Utilizing an Automated Annular Pressure Control System for Managed Pressure Drilling in Mature Offshore Oilfields". Paper SPE 96646-MS presented at the Offshore Europe, Aberdeen, United Kingdom, 09/06/2005. doi: 10.2118/96646-MS.

Reitsma, Don. 2010. A simplified and highly effective method to identify influx and losses during Managed Pressure Drilling without the use of a Coriolis flow meter. Paper SPE/IADC 130312-MS presented at the SPE/IADC Managed Pressure Drilling and Underbalanced Operations Conference and Exhibition, Kuala Lumpur, Malaysia, 24-25 February 2010.

Santos, H., Leuchtenberg, C., and Shayegi, S. 2003. "Micro-Flux Control: The Next Generation in Drilling Process". Paper SPE 81183-MS presented at the SPE Latin American and Caribbean Petroleum Engineering Conference, Port-of-Spain, Trinidad and Tobago, 04/27/2003. doi: 10.2118/81183-MS.

Santos, O., Adasani, I., Azar, J. J., and Escorihuela, F. 1995. "Determination of Casing Setting Depth Using Kick Tolerance Concept". Paper SPE 30220-MS presented at the Petroleum Computer Conference, Houston, Texas, 06/11/1995. doi: 10.2118/30220-MS.

Saponja, J., Adeleye, A., and Hucik, B. 2006. "Managed-Pressure Drilling (MPD) Field Trials Demonstrate Technology Value". Paper IADC/SPE 98787-MS presented at the IADC/SPE Drilling Conference, Miami, Florida, USA, 02/21/2006. doi: 10.2118/98787-MS.

Spencer, R., Tatsis, A., and Glass, A.W. 1999. "Kick Simulation for Well Design and Kick Management on the U.K. Continental Shelf: Current Industry Practice and Challenges for the Future". Paper SPE 56922-MS presented at the Offshore Europe Oil and Gas Exhibition and Conference, Aberdeen, United Kingdom. doi: 10.2118/56922-MS.

SPT, Scanpower Petroleum Technology. *Dynaflowdrill*^{TM} 2010. Available on http://www.sptgroup.com.

Urbieta, A., Perez-Tellez, C., C.Lupo, J.M.Castellanos, O.Ramirez, G.Puerto, and J.Bedoya. 2009. "Successful Application of MPD Technique in a HP/HT Well Focused on Performance Drilling in Southern Mexico Deep Fractured Carbonates Reservoirs". Paper IADC/SPE 122200 presented at the IADC/SPE Managed Pressure Drilling and Underbalanced Operations Conference & Exhibition, San Antonio, Texas, 02/12/2009. doi: 10.2118/122200-MS.

VanRiet, E.J., Reitsma, D., and Vandecraen, B. 2003. "Development and Testing of a Fully Automated System to Accurately Control Downhole Pressure During Drilling Operations". Paper SPE/IADC 85310-MS presented at the SPE/IADC Middle East Drilling Technology Conference and Exhibition, Abu Dhabi, United Arab Emirates, 10/20/2003. doi: 10.2118/85310-MS.

Vieira, P., Arnone, M. A., Torres, F., and Barragan, F. 2009. "Roles of Managed Pressure Drilling Technique in Kick Detection and Well Control -The Beginning of the New Conventional Drilling Way". Paper SPE/IADC 124664 presented at the SPE/IADC Middle East Drilling Technology Conference & Exhibition, Manama, Bahrain, 10/26/2009. doi: 10.2118/124664-MS.

Vieira, P., Arnone, M., Cook, I., Moyse, K., Haojie, H., Qutob, H. H., Yuesheng, C., and Qing, C. 2008. "Constant Bottomhole Pressure: Managed-Pressure Drilling Technique Applied in an Exploratory Well in Saudi Arabia". Paper SPE/IADC 113679-MS presented at the SPE/IADC Managed Pressure Drilling and Underbalanced Operations Conference and Exhibition, Abu Dhabi, UAE, 01/28/2008. doi: 10.2118/113679-MS.

Villatoro, J. J., Schmigel, K., and Boutalbi, S. M. 2009. "Controlled Pressure Drilling (CPD) Candidate Screening Methodology". Paper SPE 120035-MS presented at the SPE Middle East Oil and Gas Show and Conference, Bahrain, Bahrain, 03/15/2009. doi: 10.2118/120035-MS.

Watson, D., Brittenham, T., and Moore, P. L. 2003. *Advanced well control*, *SPE textbook series v. 10*. Richardson, Tex.: Society of Petroleum Engineers.

Appendix A Well X Simulation Input Data

Case Description

Project: Circulating studies
Data description: Simulation inputs for no kick case (Base) with high permeability
Well: X
Well section: 6 in.
Software: Drillbench (Dynaflodrill module)
Company: SPT (Scandpower Petroleum Technology) Group
Creator: Jose Chirinos
Date: 01-Aug-2009

Survey

Md [ft]	Inclination [deg]	Azimuth [deg]	Vertical depth [ft]
0	0	0	0
10074	26.4	48.8	10005.88
10349	27.7	49.2	10251.08
10623	30.9	50.4	10490.69
10895	34.4	50	10719.59
11165	37	49.3	10938.2
11435	38	49.4	11152.41
11707	39.4	49.4	11364.77
11982	40.4	49.8	11575.74
12254	40.8	50	11782.57
12531	40.6	50.4	11992.47
12805	40.2	50.6	12201.02
13175	41	50.9	12481.86
13451	41	50.9	12690.06
13727	41.5	50.8	12897.89
14002	40.8	50.7	13104.65
14233	40.8	51.3	13279.25
14503	39.9	51.3	13484.61
14772	40.4	51.4	13690.42
14862	40.1	51.5	13759.11
14951	40.1	51.7	13827.19
15042	40.1	51.7	13896.8
15132	40.2	52.1	13965.59
15170	40.2	52.2	13994.62
15193	41.6	54.4	14012.01
15200	41.6	54.4	14017.24
15243	41.6	54.4	14049.37
15300	41.1	55.3	14092.16
15400	40.1	56.8	14168.12
15443	39.6	57.4	14201.13
15500	40.7	59	14244.7
15600	42.5	61.5	14319.49
15700	44.4	63.9	14392.08
15750.7	45.4	65.1	14428.01
15800	44.9	63.4	14462.76

15900	44	60.1	14534.12
16000	43.3	56.7	14606.49
16021.3	43.1	55.9	14622.02
16100	43.1	55.9	14679.49
16200	43.1	55.9	14752.5
16300	43.1	55.9	14825.52
16400	43.1	55.9	14898.54
16500	43.1	55.9	14971.55
16580	43.1	55.9	15029.99
16600	43.1	55.9	15044.57
16700	43.1	55.9	15117.58
16780	43.1	55.9	15176.03
16800	43.4	55.9	15190.56
16900	44.9	55.9	15262.31
16982.3	46.1	55.9	15319.98
17000	46.1	55.9	15332.25
17100	46.1	55.9	15401.55
17200	46.1	55.9	15470.85
17300	46.1	55.9	15540.16
17400	46.1	55.9	15609.46
17500	46.1	55.9	15678.76
17600	46.1	55.9	15748.06
17675	46.1	55.9	15800.01

Wellbore Geometry

Name	Hanger depth [ft]	Setting depth [ft]	Inner diameter [in]	Outer diameter [in]
7" T95 32.0 lbs/ft	0.00	15150.00	6.094	7.000

Target depth (ft): 17700.00
Open hole length (ft): 1110.00
Open hole diameter (in): 6.00

String

Components	Type	Section length [ft]	Inner diameter [in]	Outer diameter [in]
DC 4 3/4" NC 35-37	DrillCollar	250	2.5	4.75
HWDP 3 1/2" NC38(3 1/2 IF)	Drillpipe	450	2.063	3.5
dp 3 1/2" S135 15.50 lb/ft	Drillpipe	15560	2.602	3.5

Average stand length (ft): 95.00
Bit outer diameter (in): 6.00
Flow area (sq in): 0.37
Number of bit nozzles: 4
Nozzles diameter (1/32 in): 11

Choke

Inner diameter (in): 3.00
Closure time (min): 0.50
Choke control: Opening
Working pressure (psi): 14.70

Mud

Type: Water Based Mud (WBM)
Base oil density (ppg): 7.3022
Water density (ppg): 8.3454
Solids density (ppg): 35.0507
Density (ppg): 13.20
Reference temperature (deg F): 90.00
Fluid type: Liquid
Oil water ratio: 0 / 100
Rheology type: Non-Newtonian; Fann tables
PVT model: Black oil

Fann Reading

Shear rate [rpm]	Shear stress [lbf/100ft2]
600	47
300	26
200	17
100	11
6	3
3	2

Reservoir

Name	Top [ft]	Bottom [ft]	Type	Press [psi]	Temp [degF]	Porosity [0-1]	Perm [mD]	Fluid	Flow model
Form1	15150	16265	Matrix	8723	145	0.27	1	Gas	Reservoir model
HP Sand	16265	16401	Matrix	10544	155.81	0.27	500	Gas	Reservoir model

Hole cleaning criterion: Max concentration
Cuttings density (ppg): 0.1
Max concentration: 0.04

Water		
Density	(ppg)	8.4289
Compressibility	(1/psi)	7.58 E-08
Volume	factor	1
Viscosity	(cp)	1

Oil		
Density	(ppg)	7.4691
Compressibility	(1/psi)	1.38 E-06
Volume	factor	1.1
Viscosity	(cp)	2

Gas	
Density (SG)	0.65
N2	0
CO2	0
Hydrocarbon	1
H2S	0

Temperature

Drillstring Temperature	
Depth [ft]	[def F]
0	85
17700	170
Annulus Temperature	
Depth [ft]	[def F]
0	90
17700	170

Optional Input

Open hole roughness: 0.099996
Steel roughness: 0.0004
Pressure loss model: Semi-empirical
Gas density model: Hall-Yarborough
Friction factor model: Dodge-Metzner
Rheology model: Robertson-Stiff

End of data.

Appendix B Example of Maximum Casing Pressure Calculation (proposed method)

Input data – Well X, 0.2 ppge circulating UB and 20 bbl kick size

Vertical depth	14800	ft		
MAASP	790	psi		
	OD	**ID**	**Depth**	
Casing	7.000"	6.094"	13979	ft
Open Hole	6.000"		821	ft
DC	4.750"	2.500"	250	ft
HW	3.500"	2.063"	450	ft
DP	3.500"	2.602"	14280	ft
Mud Density	13.2	lbm/gal		
SG	0.6			
Temperature	90°F	0.534759	°F / 100 ft	
Pump Rate	190	gpm		
Friction @ TD	507	psi		

Following the procedure described in section 6.3, peak casing pressure during circulation can be estimated as follows:

1. Depth where gas velocity > mixture velocity (Eq. 2.15)

$$V_{mix} = \frac{Pump\ rate}{2.448 * (Csg_{ID}^2 - DP_{OD}^2)} = \frac{190\ gpm}{2.448 * (6.094^2 - 3.5^2)} = 3.18\ ft/sec$$

$$V_{front} = e^{1.767 - 2.953e-4 * D}$$

$$D_1 = + \frac{1.767 - ln(V_{front})}{0.0002953} = \frac{1.767 - ln(3.18)}{0.0002953} = 2132\ ft$$

2. Front, apex and tail velocities estimation (Eq. 6.2) (Eq. 6.1)

$$V_{front} = 3.132e-8 * D_1^2 - 6.2854e-4 * D_1 + 5.8677 = 4.67\ ft/sec$$

$$V_{apex} = 4.6029e-8 * D_1^2 - 7.8566e-4 * D_1 + 5.8246 = 4.358\ ft/sec$$

$$V_{tail} = V_{mix}$$

3. Initial conditions at 2132 ft are determined by applying single bubble method (Eq. 2.8) and (Eq. 2.9)

$$P_{gas} = 3285\ psi$$

$$h_{D1} = 1363\ ft$$

4. Estimate the length of the base of the triangle (h_o) with 0:

$$h_o = 3\ h_{D1} = 3 * 1363\ ft = \ 4089.57\ ft$$

5. Estimate the time required for the leading edge to reach the surface from D_1 (Eq. 6.4):

$$t_{front} = D_1\ V_{front} = 2132\ ft * 4.67\ ft/\sec = 456.54\sec = 7.61\ min$$

6. The depths of the apex and the tail corners when the gas reaches surface are estimated as follow:

$$\text{(Eq. 6.5)}\ D_{apex} = D_1 + \frac{h_o}{2} - \ (V_{apex}\ t_{front}) = 2132\ ft + \frac{4089.57\ ft}{2} - \ (4.358\ ft/sec * 456.54\ sec)$$

$$D_{apex} = 2186.83\ ft$$

$$\text{(Eq. 6.6)}\ D_{tail} = D_1 + \ h_0 - \ (V_{tail}\ t_{front}) = 2132\ ft + \ 4089.57\ ft - \ (3.118\ ft/sec * 456.54\ sec)$$

$$D_{tail} = 4797.77\ ft$$

7. Gas volume at depth D_{apex} is estimated applying gas law as for single bubble (Eq. 2.8) and (Eq. 2.9)

$$P_{gas}@\ D_{apex} = 3050\ psi$$

$$h_{gas}@\ D_{apex} = 1450\ ft$$

$$V_{D\ apex} = 35.05\ bbl$$

8. Average gas fraction is equal to (Eq. 6.7):

$$\alpha_{average} = \frac{V_{D\ apex}}{A_{an} D_{tail}} = \frac{35.05\ bbl * 5.64158\ ft^3/bbl}{0.136\ ft^2 * 4797.77\ ft}$$

$$\alpha_{average} = 0.3022$$

9. Maximum gas fraction 0:

$$\alpha_{max} = 2\ \alpha_{average} = 0.604$$

10. The equivalent hydrostatic loss when the apex corner reaches the surface is then estimated as (Eq. 6.9):

$$\Delta P_{hyd} = 0.052\ EMW\ \frac{\left[\left(D_{tail} - \ D_{apex}\right)\ \alpha_{max}\right]}{2} - P_{hg}$$

$$P_{hg} = \frac{\gamma_g \, p \, h_k}{53.29 \, z \, T} = \frac{0.6 * 3050 \, psi * 789 \, ft}{53.29 * 0.8233 * (460 + 101.7)} = 58.58 \, psi \quad \text{(Eq. 2.6)}$$

$$\Delta P_{hyd} = 0.052 * 13.2 * \frac{[(4797.77 \, ft - \, 2186.83 \, ft) \, 0.604]}{2} - 58.58 \, psi$$

$$\Delta P_{hyd} = 480.47 \, psi$$

11. Maximum casing pressure during kick circulation is estimated as follow (Eq. 6.10):

$$CP_{max} = \Delta P_{hyd} + \Delta P_{UB}$$

$$CP_{max} = 480.47 \, psi + 0.2 \, ppge * 0.052 * 14800 \, ft$$

$$CP_{max} = 634.39 \, psi$$

Appendix C Full Scale Experiment LSU "B" No.7 Well (CP_{max})

Additional full scale data were used to estimate maximum casing pressure (CP_{max}) with the proposed method. The LSU "B" No.7 well was extensively used in the 70's and the 80's to train industry personnel in proper methods of well control at LSU. Figure C1 shows a schematic of the training well. The casing is 5 ½", 17 lb/ft, J-55 pipe cemented at 6140 ft. Simulating the drill pipe is 2 7/8", 6.5 lb/ft, J-55 tubing, run to a depth of 6011 ft. A 1" injection line, run inside the 2 7/8" tubing to a depth of 6029 ft, is use to simulate a gas kick.

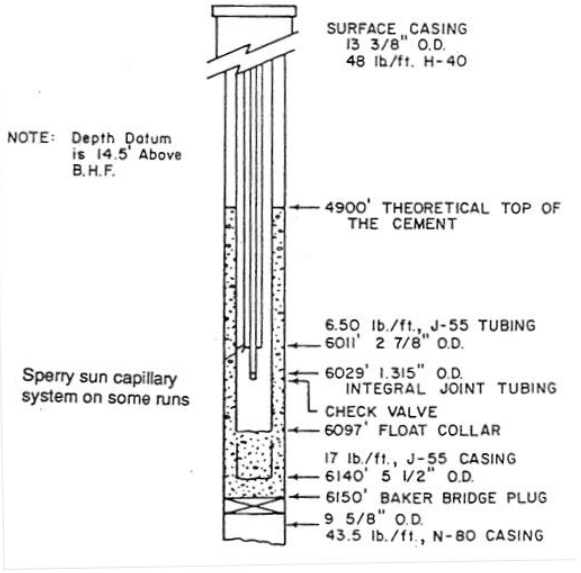

Figure C1 Schematic of LSU "B" No.7

Data from four full scale well control experiment performed in 1972 were used to evaluate the performance of the proposed method in a different well geometry.

Test No.	Date	Description	MW (ppg)	PV (cp)	YP ($lb/100ft^3$)	Kick Size (bbl)	SIDP (psia)	SICP (psia)	Kill Rate (bbl/min)
1	4/12/72	Well control simulation	8.6	12.6	15	10	N.R	515	2.3
2	4/25/72	Well control simulation	8.6	3.5	2.5	10.3	405	660	2.3
3	4/25/72	Well control simulation at very slow kill speed	8.6	3.5	2	10	455	745	1.19
4	10/24/74	Well control simulation after extended shut-in period	8.6	13.5	5.5	10	190	398	2.3

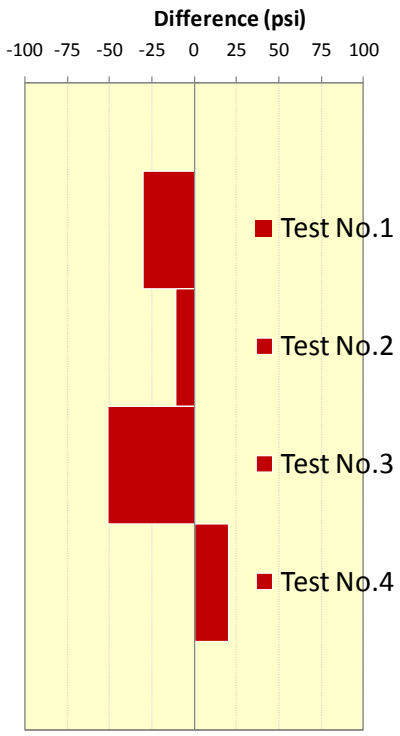

Figure C2 Comparison CP_{max} LSU #1

Table C1 Results CP_{max} LSU #1

Test	Actual CP_{max}	Estimated CP_{max}	Cp_{max} after SF	Diff. (psi)	Diff (%)
Test No.1	850	683	820	-30	-3.71%
Test No.2	880	790	869	-11	-1.27%
Test No.3	1035	856	985	-50	-5.14%
Test No.4	555	523	575	20	3.53%

Figure C2 and Table C1 show the results after comparing the actual and the estimated CP_{max}. CP_{max} was estimated using the method described in Chapter 6 and the safety factor in Table 6.1. The estimates generally under predicted the actual CP_{max}, by as much as 51 psi or 5.1% in test No. 3. The main characteristic of Test No. 3 is that they used a very slow kill pump rate of 1.19 bbl/min (49.98 gpm). It can be concluded that the proposed method is sensitive to annular velocity and possibly annulus size during kick circulation. However, the proposed method achieved a reasonable agreement with the experimental data.

Appendix D Results Maximum Casing Pressure Estimation

Simulated Kick Scenarios

	Well X (190 gpm)	Well Y (760 gpm)	LSU #2 (195 gpm)
Static BHP (psi)	10186	13275	2617
Circulating BHP (psi)	10706	13464	2942
Friction (psi)	520	189	325

Simulated Cases	**X1**	**X2**	**X3**	**Y1**	**Y2**	**Y3**	**L1**	**L2**	**L3**
P_f (psi)	10860	11289	11555	13606	14000	14245	3096	3525	3790
Static UB (psi)	674	1103	1369	331	725	970	479	908	1173
Circulating UB (psi)	154	583	849	142	536	781	154	583	848
Kick intensity (ppge)	**0.20**	**0.76**	**1.10**	**0.18**	**0.69**	**1.00**	**0.50**	**1.91**	**2.77**

Well X			**Peak Casing Pressure (psi)**			**Difference**	
Circ. UB	**Case**	**Pit Gain**	**DFD[1]**	**SB[2]**	**PM[3]**	**Press. (psi)**	**Perce. (%)**
0.20 ppge	X1	2 bbl	465	989	559	94	16.86%
		10 bbl	845	1573	761.3	-84	-10.99%
		20 bbl	1150	2024	876	-274	-31.23%
0.76 ppge	X2	2 bbl	875	1332	916.3	41	4.51%
		20 bbl	1520	2292	1259.3	-261	-20.70%
1.10 ppge	X3	2 bbl	1115	1562	1150.3	35	3.07%
		10 bbl	1425	2046	1372.3	-53	-3.84%
		20 bbl	1775	2473	1499.3	-276	-18.39%

[1]DFD: maximum casing pressure estimated by computer simulation
[2]SB: maximum casing pressure estimated by single bubble calculation
[3]PM: maximum casing pressure estimated by the proposed method

Well Y			**Peak Casing Pressure (psi)**			**Difference**	
Circ. UB	**Case**	**Pit Gain**	**DFD[1]**	**SB[2]**	**PM[3]**	**Press. (psi)**	**Perce. (%)**
0.18 ppge	Y1	2 bbl	260	451	296	36	12.16%
		10 bbl	430	855	504	74	14.68%
		20 bbl	596	1160	592	-4	-0.68%
0.69 ppge	Y2	2 bbl	654	753	694	40	5.76%
		20 bbl	930	1399	933	3	0.32%
1.00 ppge	Y3	2 bbl	899	967	922	23	2.49%
		10 bbl	1425	2046	1372.3	57	5.39%
		20 bbl	1775	2473	1499.3	-13	-1.13%

LSU#2			Peak Casing Pressure (psi)			Difference	
Circ. UB	**Case**	**Pit Gain**	**DFD[1]**	**SB[2]**	**PM[3]**	**Press. (psi)**	**Perce. (%)**
0.5 ppge	L1	2 bbl	446	550	455	9	1.98%
		10 bbl	666	766	605	-61	-10.08%
		20 bbl	870	943	782	-88	-11.25%
1.91 ppge	L2	2 bbl	825	945	871	46	5.28%
		20 bbl	1245	1268	1134	-111	-9.79%
2.77 ppge	L3	2 bbl	1060	1200	1132	72	6.36%
		10 bbl	1340	1342	1231	-109	-8.85%
		20 bbl	1400	1485	1363	-37	-2.71%

Appendix E Computer Simulations (Examples)

Well X

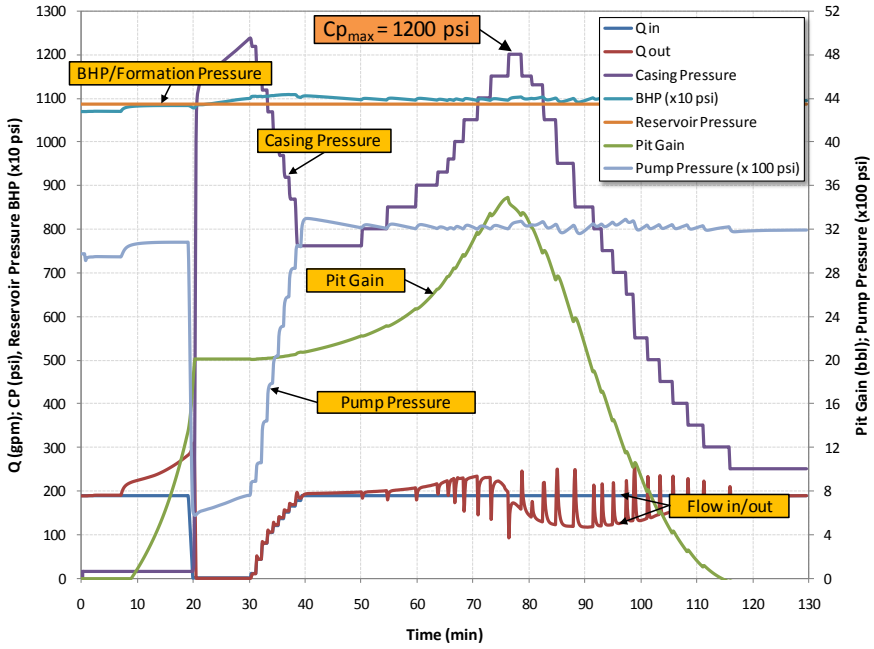

Non-circulating responses on 20 bbl kick 0.2 ppge circ. UB (Full Rate)

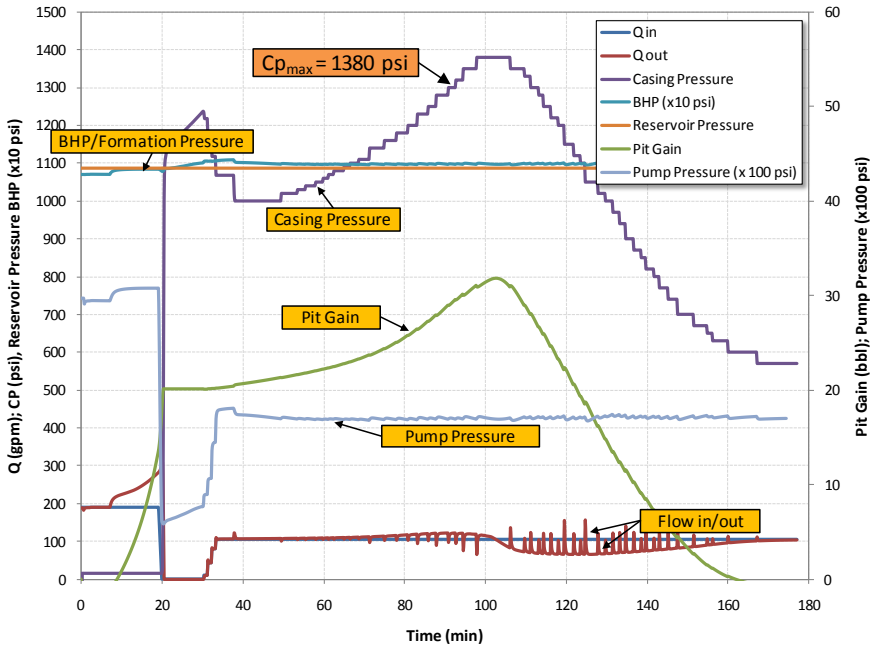

Non-circulating responses on 20 bbl kick 0.2 ppge circ. UB (Reduced Rate)

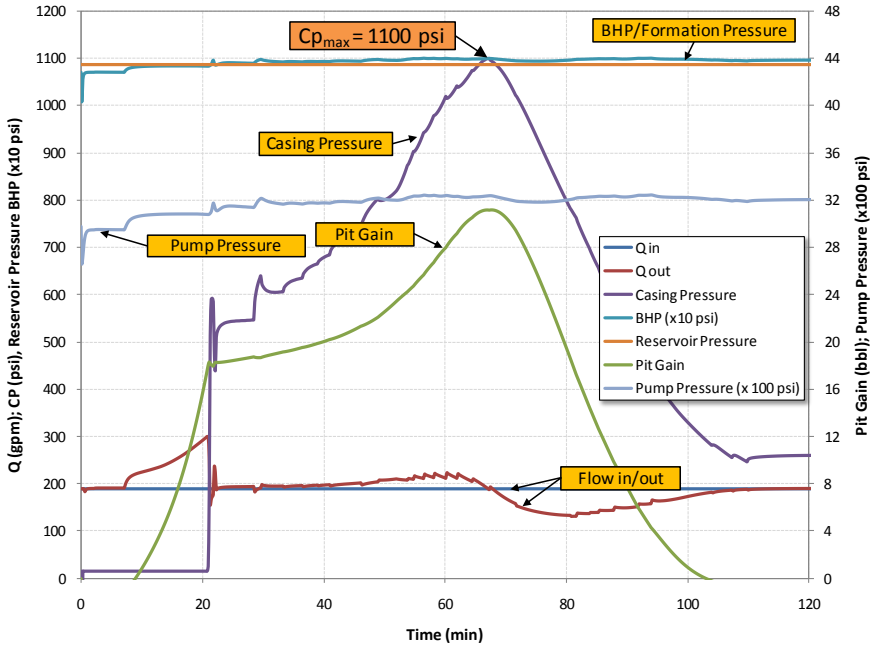

Circulating response on 2 bbl kick 0.5 ppge circ. UB

Well Y

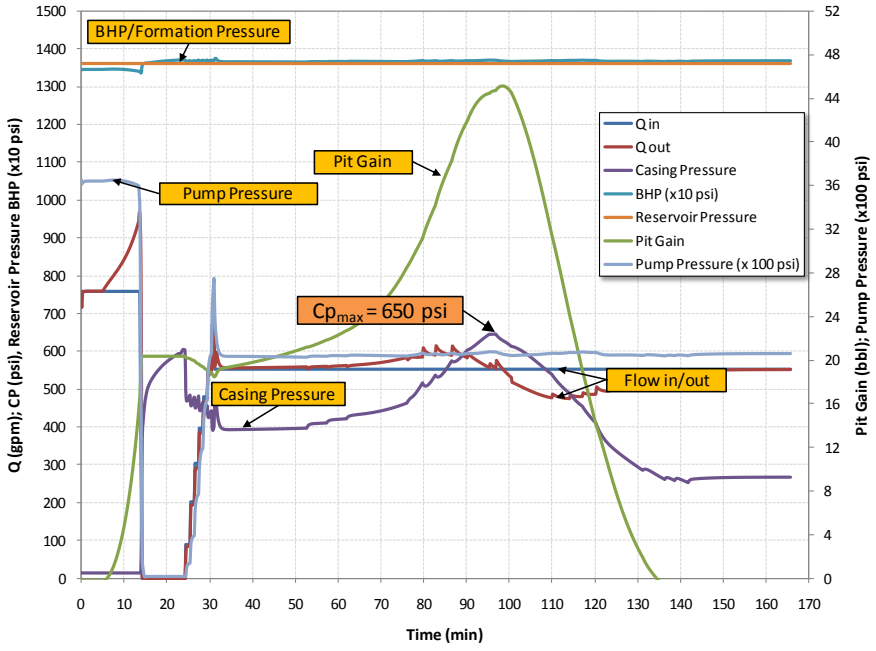

Non-circulating responses on 20 bbl kick 0.18 ppge circ. UB (Full Rate)

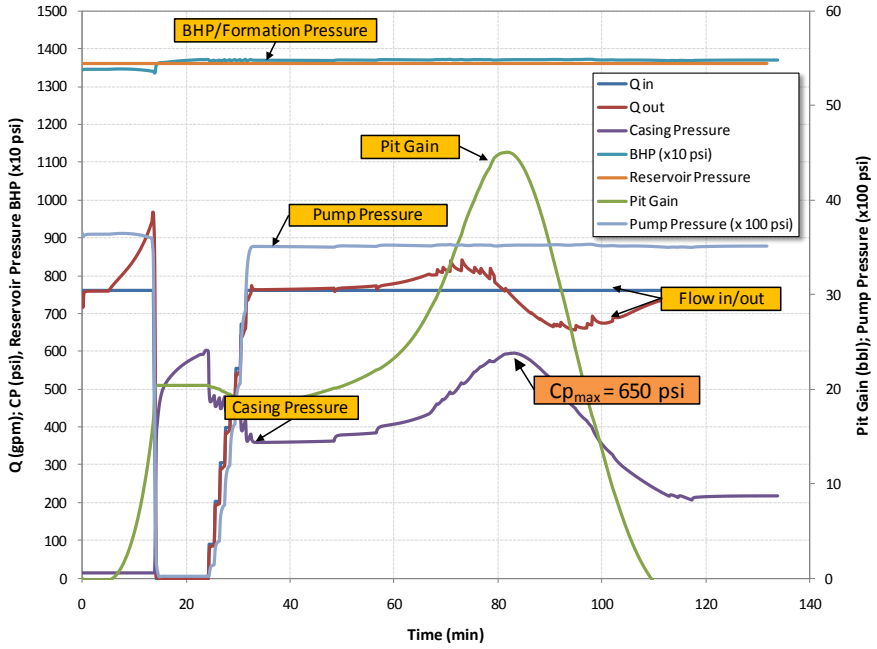

Non-circulating responses on 20 bbl kick 0.18 ppge circ. UB (Reduced Rate)

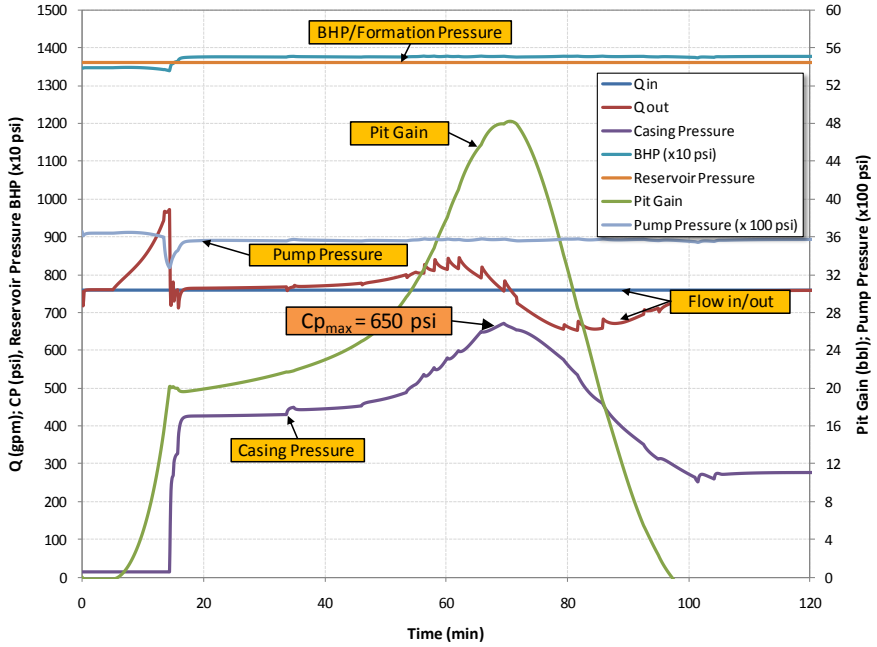

Circulating response on 2 bbl kick 0.5 ppge circ. UB

LSU #2

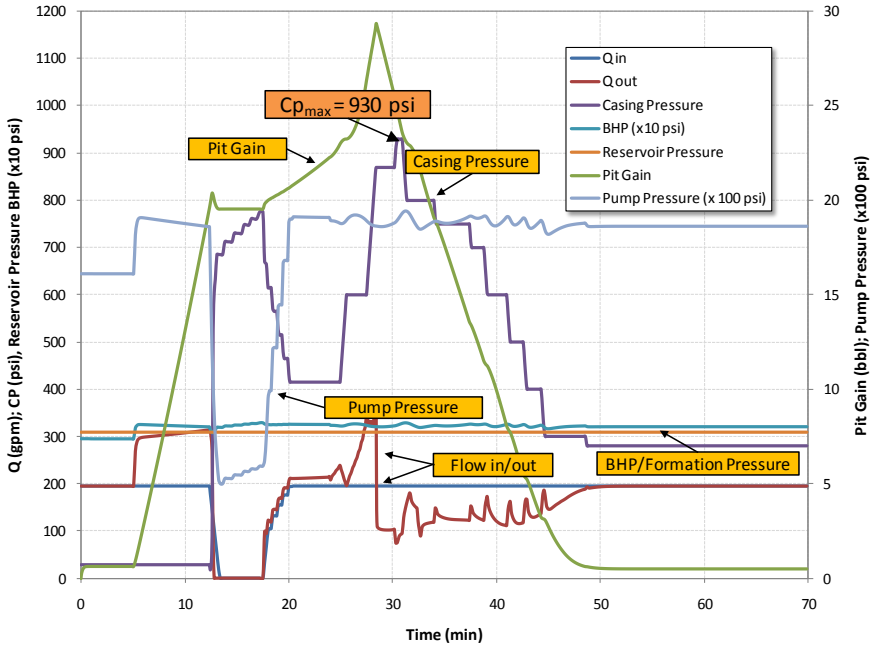

Non-circulating responses on 20 bbl kick 0.5 ppge circ. UB (Full Rate)

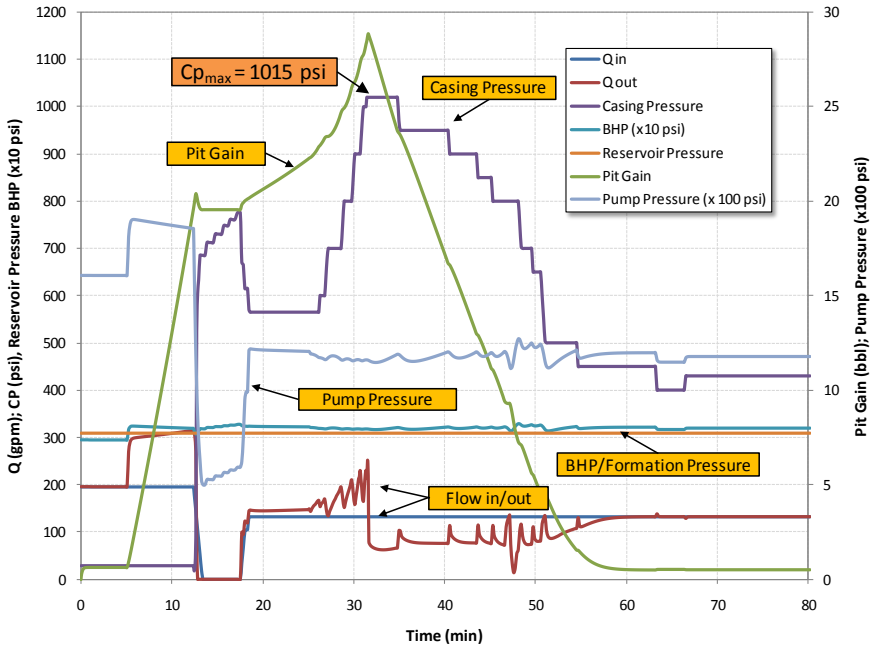

Non-circulating responses on 20 bbl kick 0.5 ppge circ. UB (Reduced Rate)

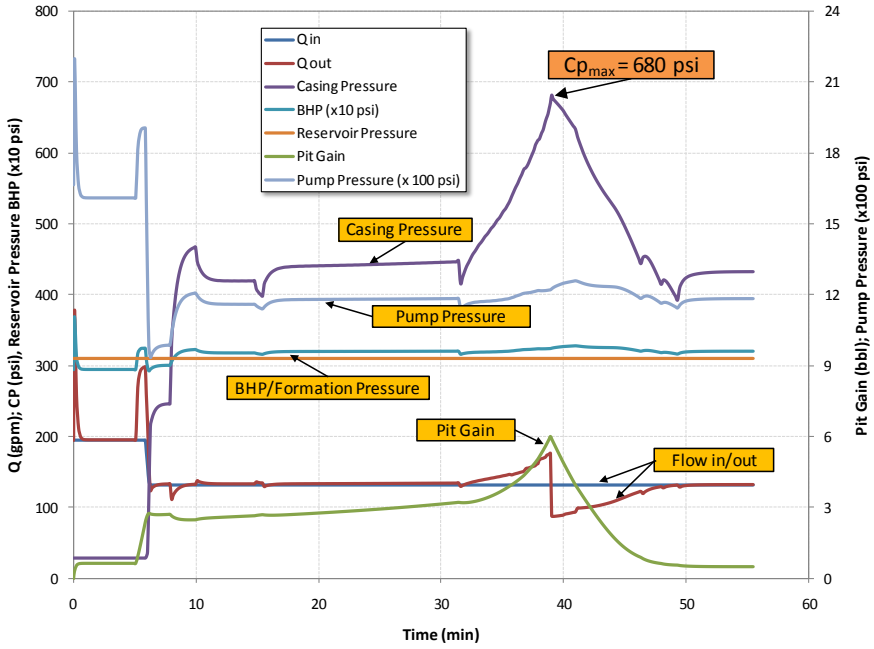

Circulating response on 2 bbl kick 0.5 ppge circ. UB

Vita

José E. Chirinos was born in Caracas, capital of Venezuela, in 1980. He received his Bachelor of Science degree in petroleum engineering in 2004 from Universidad Central de Venezuela UCV (Central University of Venezuela). José was employed first as intern for six months, and then as full time engineer for 4.5 years by Vinccler Oil and Gas. He worked as drilling, completion and workover engineer in Falcon State, Venezuela. In 2008, he decided to further his education by entering the master's program in petroleum engineering at Louisiana State University (LSU). His interests include drilling and production engineering, flow modeling, managed pressure drilling, well design and optimization.